Fish and Shellfish Immunology 145 (2024) 109319

Contents lists available at ScienceDirect

Fish and Shellfish Immunology

journal homepage: www.elsevier.com/locate/fsi

Transcriptome profiling of microdissected cortex and medulla unravels functional regionalization in the European sea bass *Dicentrarchus labrax* thymus

A. Miccoli [a], V. Pianese [b], C. Bidoli [c], A.M. Fausto [b], G. Scapigliati [b], S. Picchietti [b,*]

[a] National Research Council, Institute for Marine Biological Resources and Biotechnology (IRBIM), 60125, Ancona, Italy
[b] Dept. for Innovation in Biological, Agro-food and Forest Systems (DIBAF), University of Tuscia, Largo Dell'Università Snc, 01100, Viterbo, Italy
[c] Dept. of Life Sciences, University of Trieste, 34127, Trieste, Italy

ARTICLE INFO

Keywords:
Laser capture microdissection
T cell development and education
Positive and negative selection
Autophagy and apoptosis
Adaptive immunity

ABSTRACT

The thymus is a sophisticated primary lymphoid organ in jawed vertebrates, but knowledge on teleost thymus remains scarce. In this study, for the first time in the European sea bass, laser capture microdissection was leveraged to collect two thymic regions based on histological features, namely the cortex and the medulla. The two regions were then processed by RNAseq and in-depth functional transcriptome analyses with the aim of revealing differential gene expression patterns and gene sets enrichments, ultimately unraveling unique micro-environments imperative for the development of functional T cells.

The sea bass cortex emerged as a hub of T cell commitment, somatic recombination, chromatin remodeling, cell cycle regulation, and presentation of self antigens from autophagy-, proteasome- or proteases-processed proteins. The cortex therefore accommodated extensive thymocyte proliferation and differentiation up to the checkpoint of positive selection.

The medulla instead appeared as the center stage in autoimmune regulation by negative selection and deletion of autoreactive T cells, central tolerance mechanisms and extracellular matrix organization.

Region-specific canonical markers of T and non-T lineage cells as well as signals for migration to/from, and trafficking within, the thymus were identified, shedding light on the highly coordinated and exquisitely complex bi-directional interactions among thymocytes and stromal components. Markers ascribable to thymic nurse cells and poorly characterized post-*aire* mTEC populations were found in the cortex and medulla, respectively. An in-depth data mining also exposed previously un-annotated genomic resources with differential signatures.

Overall, our findings contribute to a broader understanding of the relationship between regional organization and function in the European sea bass thymus, and provide essential insights into the molecular mechanisms underlying T-cell mediated adaptive immune responses in teleosts.

1. Introduction

Significant evolutionary events linked to the invasion of recombination-activating genes (RAG) and two rounds of whole genome duplication [1–6] originated the adaptive immune system in jawed vertebrates, which is centered on lymphocytes with a vast immune repertoire [7,8] and gifted by high degree of specificity towards pathogens and long-term immunological memory [9].

Jawed vertebrates use lymphocytes uniquely capable of somatic recombination of immunoglobulin (Ig)-related genes codifying for antibody classes and T cell receptor (TCR) complexes [9]. Their lymphocytes differentiate and mature from hematopoietic precursors in specialized sites in the animal's body, namely primary lymphoid tissues [10], which exhibit and commit to a remarkable functional dichotomy of lineages [11]: B cell repertoire generates in Leydig's and epigonal organs/head kidney/*bursa of Fabricius*/bone marrow [12,13] (locations that considerably differed along phylogeny and ontogeny), while T cell repertoire generates exclusively in the thymus [14].

The thymus is a sophisticated anatomical structure that emerged early in the history of vertebrates. It was seen first in a primitive form, namely the thymoids, in jawless fish [15] but gained complexity in cartilaginous fish, the first group to have a true thymus [16], and

* Corresponding author. Department for Innovation in Biological, Agro-food and Forest systems, University of Tuscia, Largo dell'Università, I-01100, Viterbo, Italy.
E-mail address: picchietti@unitus.it (S. Picchietti).

https://doi.org/10.1016/j.fsi.2023.109319
Received 27 October 2023; Received in revised form 15 December 2023; Accepted 18 December 2023
Available online 23 December 2023

continued through vertebrate evolution [13]. The organ underwent diverse, although related, developmental patterns across vertebrate classes [17], maintaining its primary and crucial role in providing specialized immunological niches for T development [16,18,19]. The outcome is the generation of mature T cells that express a self-tolerant repertoire of somatically diversified antigen receptors [20].

The thymus is a paired organ that derives from a primordium in the pharyngeal pouches of the endodermal gut tube (foregut endoderm). The neural crest-derived mesenchyme provides precious support to the process, acting as the mediator for the functional development of thymic epithelial cells and contributing to form both the capsule and the intra-organ meshwork structure mingled with epithelial cells [14,21,22]. In bony fish, the thymus derives from the third pharyngeal pouch during embryogenesis and remains throughout the entire lifespan, although age associated involution has been observed in several fish species [17].

Notably, teleosts stand out as the only vertebrate group in which the organ remains closely connected to the pharynx, from which it does not detach, separate or migrate throughout adulthood [21,23], contrary to what occurs in mammals and birds [24].

Species-specific variations in the morphology and histology of the teleost thymus were reported [17,25,26]. It is a paired organ located in the gill cavity and covered by the pharyngeal epithelium [27] and can range from only one lobule as in zebrafish and medaka [28] to multi-lobed structures in other teleost fish as the European sea bass *Dicentrarchus labrax* [29]. The development, maturation, and selection of T cells is supported by stromal cells, which include non-T-lineage populations.

In *D. labrax*, we have so far studied this organ using a combination of morphological, molecular, cellular and functional analyses to elucidate the transcription, localization, distribution and role of crucial immune-related genes and proteins, also along the thymus ontogeny (e.g. Refs. [30–36]) Some of the works have strongly suggested not only anatomical but also a functional regionalization within the organ; a distinct spatial organization is already distinguishable at larval stages [37–39] and, specifically, a cortical area has been identified in the outer zone of the organ while the medulla is observed in the inner zone (e.g. Refs. [29, 37–41]).

In the present study and for the first time to the best of our knowledge, a laser-capture microdissection protocol was optimized for identification, capture and preservation of, and nucleic acid purification from, medullary and cortical thymic regions of juvenile European sea bass. In the last three decades, *D. labrax* has been increasingly employed as an experimental marine model in immunology-related research [42], yet it still suffers from fragmentary mechanistic information and mammalian paradigms with regards to origin, cellular composition and function, as well as to the relevance of microenvironments governing the organ behavior, T cell development and immune status. It also lacks high-throughput sequencing data of enriched stromal and lymphoid populations from *a priori* defined thymic regions.

The findings we present contribute significantly to advancing our understanding of gene expression within distinct thymic microenvironments. Through our comprehensive spatial mapping efforts, we have identified gene clusters that define each cortical and medullary region, and uncovered key pathways involved in functional T lymphocyte development, thymocyte migration, immune tolerance and homeostasis via supportive and inductive thymic microenvironments. We believe these results are relevant to lay the groundwork for additional studies aimed at further characterizing the evolutionary biology of teleost adaptive immunity.

2. Methods

2.1. Histology and laser microdissection

Both thymi were collected from 1-year old European seabass *Dicentrarchus labrax* specimens and were either fixed in ice-cold Bouin's fixative for 7 h at 4 °C and gradually dehydrated before paraffin wax embedding for histological analyses (n = 2) or included in Kilik-BioOptica OCT (BioOptica, IT) and frozen in liquid nitrogen for laser microdissection (n = 3).

Serial 7 μm-thick sections were cut using a rotary microtome, collected on poly-L-lysine coated slides, air-dried overnight at 37 °C and stained with May-Grünwald/Giemsa (MGG) (Pappenheim method) for general histology [31]. The obtained sections were examined under a Zeiss microscope equipped with a color 8 video camera (Axio Cam MRC) and a software package (AxioVision).

Transverse 8 μm-thick sections were cut at Leica Biosystems CM 1510-1 cryostat and posed on membrane based polyethylene naphthalate (PEN) glass slides (cat. # 11505189, Leica Microsystems). Membrane slides were previously sterilized by a 15-min immersion in RNase AWAY™ followed by a 2-min immersion in molecular grade H_2O, 2-min immersion in 100 % sterile ethanol and 45-min irradiation to UV-C (254 nm). Tissue sections were fixed in cold 75 % ethanol at −20 °C, rinsed in RNase-free water for 1 min for OCT removal and gradually dehydrated in 75 %, 90 % and 100 % ethanol washes for 30 s each. A 1-min incubation was performed in a modified Cresyl violet staining solution (i.e. 0.5 g Cresyl violet in 50 mL 100 % ethanol) recommended for RNA-based research as the lack of any PBS or water steps in stain solution preparation prevent degradation of RNA by humidity-activated RNases. A final 3-min fixation step in 100 % ethanol was then applied before allowing the sections to air dry for 1 min. Sections selected for microdissection were chosen based on the presence of intact cortical and medullary regions. Cortical and medullary thymic zones were visualized and microdissected using a Leica LMD6 microdissection system equipped with a motorized stage and a Leica CC7000 camera. All steps along the workflow were appropriately modified, with particular regards to fixation and RNA purification in case of transcriptomics-based microdissection studies [43]. Microdissected samples were gravity-collected into collection caps that had been previously sterilized by 10-min rinse in 3 % H_2O_2 followed by a 2-h immersion in Diethyl pyrocarbonate (DEPC)-treated water at 37 °C, autoclaving and irradiation to UV-C light. A minimum cumulative area of 10×10^6 μm^2 per thymic region per replicate was collected to ensure adequate RNA yields as per preliminary RNA isolation protocol optimization trials. The cortex and medulla microdissected from each of the biological triplicates were used for RNAseq. Microdissected samples were stored at −80 °C until RNA preparation.

2.2. RNA preparation and sequencing

Total RNA was extracted using the QIAGEN RNeasy Micro kit following the manufacturer's protocol. The quality and quantity of the extracted RNA was determined by the RNA 6000 pico assay (cat. # 5067–1513, Agilent Technologies) on a Bioanalyzer 2100 (Agilent Technologies). Only RNA samples associated with RNA Integrity Numbers (RINs) above 7 were maintained for downstream processing.

mRNA library preparation, scaled down to the low-input protocol variant of the Quant seq 3′-term kit (Lexogen), and sequencing on an Illumina NextSeq 500 platform with a 1 × 75 single-end sequencing strategy and a depth of 1 × 5 M reads per sample, were outsourced to BMR Genomics (Padua, Italy).

2.3. RNAseq data processing

Raw sequencing data, deposited into the NCBI SRA database under the BioProject accession number PRJNA1001662, were imported into the CLC Genomics Workbench software (v.22.02.2) and trimmed to remove residual adapters, low-quality nucleotides (nt) with a base caller quality threshold set at 0.05, ambiguous nt, poly(A) and poly(G) sequences, and homopolymers from the 3′ end. One and 13 nt were trimmed off from the 3′ and 5' end, respectively, to remove a compositional bias observed from a quality control previously conducted.

Trimmed reads were mapped to the annotated reference *D. labrax* genome available at Ensembl Genome Browser (dlabrax2021, GCA_905237075.1), release 109 (Feb. 2023), using the "RNA-Seq Analysis" tool of CLC Genomics Workbench. Mapping parameters were set as follows: "Mismatch cost" = 2; "Insertion cost" = 3; "Deletion cost" = 3; "Length fraction" = 0.95; "Similarity fraction" = 0.98.

2.4. Differential gene expression and functional analyses

Differentially expressed genes between the two thymic regions were detected by means of a negative binomial generalized linear model using the R *DESeq2* package, v. 1.40.1 [46] setting the cortex as reference level. Raw estimated counts of sequencing reads were normalized to sequencing depth and RNA composition with the median of ratios method, which is recommended for gene count comparisons between samples and for DE analysis. A minimal pre-filtering step of lowly-expressed genes step was applied to only maintain genes with a sum of reads across both thymic regions of at least 3 for i) memory size and processing time reduction and ii) increased statistical power of DEGs detection [47]. An independent filtering based on the mean of normalized counts for each gene was applied with a false discovery rate (FDR) cutoff of 0.05. Genes displaying extreme outliers and below the low mean threshold were filtered out from the dataset. Log_2 fold change estimates were tested for statistical significance using the Wald test, with the null hypothesis of no differential expression across the two regions (i.e. LFC = 0) for each gene. Log_2 fold changes were shrunk using the *apeglm* method, v. 1.22.0 [48] for visualization purposes.

Gene annotations (i.e. *D. labrax* Ensembl gene identifiers to *D. labrax* gene name, Gene Ontology mapping and *Danio rerio* Ensembl gene identifiers) were obtained from BioMart using the *biomaRt* package, v. 2.56.0 [49]. Specifically, to the latter purpose, "drerio_homolog_ensembl_gene" and "drerio_homolog_orthology_type" attributes were retrieved and, given the duplication rate in the zebrafish genome, only a one-to-one orthology mapping was maintained for downstream functional analysis.

Functional analyses were conducted with *clusterProfiler*, v. 4.8.1 [50], *ReactomePA* v. 1.44.0 [51], and visualized with *enrichplot* v. 1.20.0 [52] and *pathview* v. 1.40.0 [53].

Over-representation analyses of DEGs were conducted using *D. labrax* (function "enricher") and *D. rerio* (function "enrichGO") GO annotation, considering all genes tested for significance by *DESeq2* as background dataset (i.e. universe) for hypergeometric testing. Enriched GO terms found using *D. labrax* and *D. rerio* annotation were compared to validate the subsequent bioinformatic approach that made only use of *D. rerio* annotations.

Gene Set Enrichment Analyses [54] on KEGG (function "gseKEGG") and Reactome (function "gsePathway") pathways were run using *D. rerio* Entrez gene identifiers, whose mapping to Ensembl gene IDs was obtained via the *org.Dr.eg.db* package v. 3.17.0 [55]. To this purpose, the entire list of genes tested for significance by *DESeq2* was pre-ranked by the formula sign(log_2FC) * (-log_{10}(p-value)) as per Reimand et al. [56], and sorted in descending numerical order. The significance FDR threshold was set at 0.1.

A signaling pathway impact analysis [57], combining evidence from over-representation analysis and the actual perturbation on a given pathway, was conducted with *SPIA* v. 2.52.0 [58] using the set of Entrez ID-annotated DE genes and their log_2 fold changes estimates, together with *D. rerio* pathways topology generated from up-to-date manually-retrieved KEGG xml datasets (downloaded in June 2023). The number of bootstrap iterations for computing the probability of pathway perturbation was set to 2000.

A punctiform validation of gene expression was conducted by cDNA reverse transcription using SuperScript™ IV VILO™ Master Mix with ezDNAse (Thermo Fisher, cat. # 11766050) and qPCR assays using SSoAdvanced™ Universal SYBR® Green Supermix (BioRad cat. # 1725270). Primer pair sequences (forward and reverse in 5′-3′ direction) were: GGATGAGTCAGACCATGAG and GTGCAGATATGGGTGGAC (*rag-1*); GACGGACGAAGCTGCCCA and TGGCAGCCTGTGTGATCTTCA (*TCRβ*); GTGATAACGCTGAAGATCGAGCC and GAGGTGTGT-CATCTTCCGTTG (*CD4*); GATTCAGGCACCTACGAG and GATAC-GAAAAGCTCGAATAAC (*CD83*); CCAACGAGCTGCTGACC and CCGTTACCCGTGGTCC (*18S rRNA*) [44,45]. 0.6 ng of cDNA template were used in each PCR reaction, and amplification protocols are detailed in Refs. [44,45]. The specificity of amplification products was evaluated by dissociation curve analysis.

2.5. Sequence analysis

Targeted in-depth genome mining against custom-built and NCBI non-redundant protein sequences database was performed with the BLAST + suite v. 2.9.0 (*blastp* and *tblastn*) [59] and the NCBI BLAST web interface (*blastx*) (https://blast.ncbi.nlm.nih.gov/Blast.cgi).

Protein domain architecture and features were predicted using the simple modular architecture research tool SMART [60] (https://smart.embl-heidelberg.de/) and InterPro [61] (https://www.ebi.ac.uk/interpro/).

3. Results

3.1. Histological organization and laser microdissection of D. labrax thymus

The thymic parenchyma of 1-year old *Dicentrarchus labrax* specimens appeared surrounded by a connective capsule from which trabeculae incompletely subdivided the organ into lobules. Within each lobule, a clear histological distinction between outer (i.e. cortex) and inner (i.e. medulla) thymic compartments was evident. The cortex displayed a higher lymphoid cell density and a more compact organization pattern compared to the medulla in sections stained either with Pappenheim or Cresyl violet methods (Fig. 1A–B).

Such histological contrast was exploited for collecting the two thymic regions by laser microdissection (Fig. 1C–D, Video S1).

3.2. RNAseq data processing and transcriptome mapping

A total of 18,775,170 and 17,349,080 raw reads were obtained from the sequencing of microdissected cortex and medulla samples, with an average length of 75.3 and 75.28 bp, respectively, in accordance with the sequencing strategy employed. Following trimming, a total of 36,064,385 clean reads were generated, with a mean of 6,245,676 (99.79 % of raw data) and 5,775,785.67 (99.87 % of raw data) and an average length of 59.59 and 59.41 bp per cortex and medulla replicates. Overall, 83.84 % (84.28 % cortex, 83.41 % medulla) of the trimmed reads mapped to the reference Ensembl genome, v. 109 (February 2023). Detailed statistics on raw, processed and mapped data is available in Table 1.

3.3. Differential gene expression analysis

The mapping of trimmed RNAseq reads onto the *D. labrax* genome yielded gene expression data for 24842 annotated genes. Following a minimal pre-filtering step where only genes whose read count was greater than 3 across both thymic regions were maintained, the dataset was reduced to 16264 annotated genes.

A principal component analysis was conducted to identify possible technical batch effects of RNA isolation, library preparations and RNA sequencing. Based on 500, 1000 and 2000 genes associated with the greatest count variance across samples, the thymic region factor described the 88 %, 86 % and 85 % of the variance, with principal component 1 explaining 77, 74 and 70 % of the variance, respectively. Samples clustered strongly within tissue type in the 2D space (data not shown).

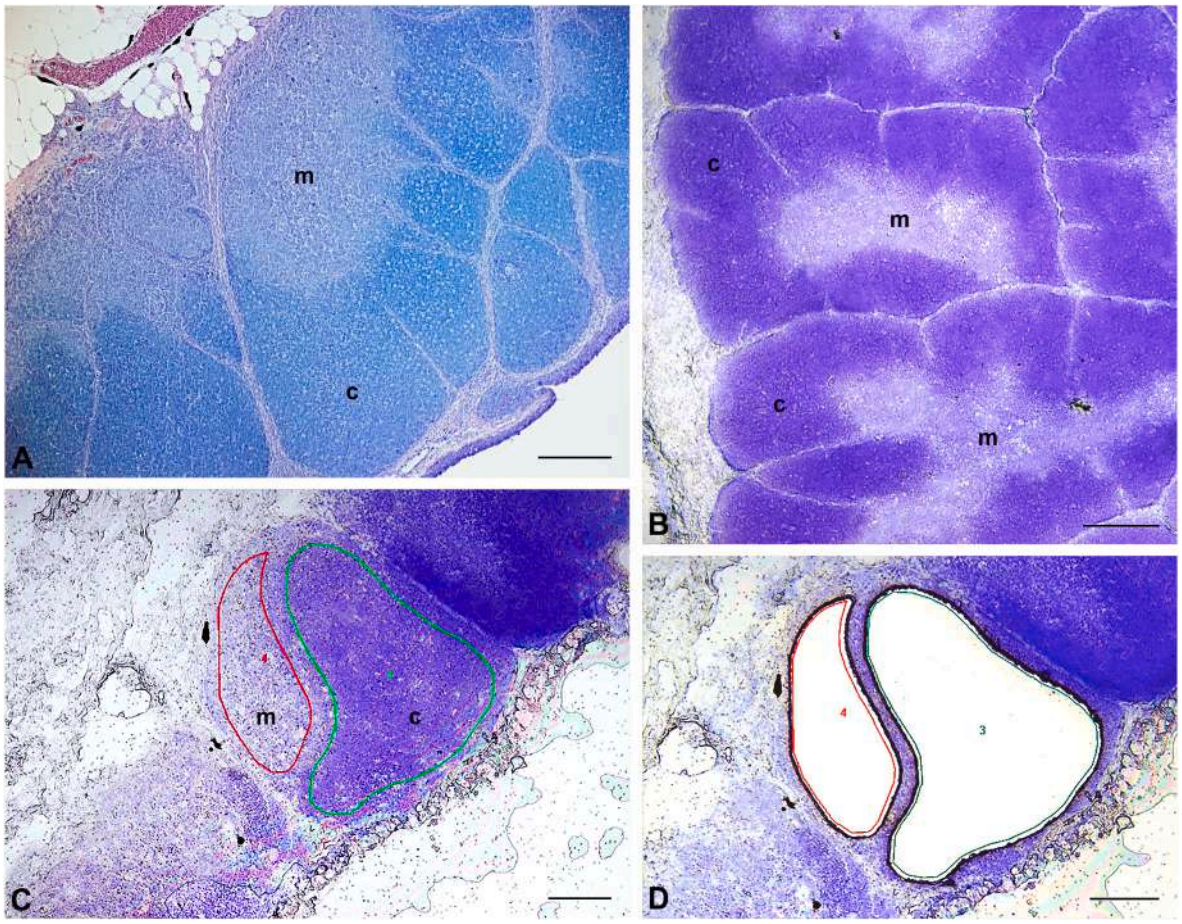

Fig. 1. Histological organization of the thymus from 1-year old *Dicentrarchus labrax*. Sections stained with either Pappenheim (A) or Cresyl violet (B) methods showing the thymic parenchyma subdivided into lobules and the greater density of lymphoid cells of the cortex (c) compared to the medulla (m). Higher magnification of a thymic lobule before (C) and after (D) laser microdissection. Scale bars of A) and B): 200 μm; scale bars of C) and D): 100 μm.

Table 1
Detailed statistics on raw, processed and mapped data.

Sample name	Raw reads (n°)	Reads after trimming (n°)	Avg. length (bp)	Avg.length after trim (bp)	Mapped (%)
T1C	6,032,749	6,027,563	75.3	59.68	84.89
T2C	5,779,711	5,776,892	75.28	59.63	83.97
T3C	6,962,710	6,932,573	75.34	59.46	83.99
T1M	5,179,402	5,173,550	75.26	59.14	82.69
T2M	6,549,969	6,537,779	75.2	58.74	82.64
T3M	5,619,709	5,616,028	75.38	60.36	84.91

The DE analysis conducted by setting a 0.05 FDR threshold identified 3154 low count genes and 6 extreme outliers, which were excluded from statistical testing. Of the remaining 13104 genes, 2373 (18.1 % of the total) resulted as differentially expressed, with thymic regionalization (i.e. medulla vs. cortex) being stronger on gene over-expression: 1458 and 915 genes were over-expressed and under-expressed in the medulla compared to the cortex, respectively (Fig. 2A). The 40 most differentially expressed genes (i.e. lowest adjusted p-value) had a statistical support ranging between 2.19E-79 (ENSDLAG00005022163 - *zinc finger protein Gfi-1b-like*, $\log_2$FC −4.43) and 5.83E-29 (ENSDLAG00005027705 - *rhoh*, $\log_2$FC −2.17), and 15 of them were over-expressed in the medulla (Fig. 2B). Twenty-one of these top DE genes were not annotated in the European seabass Ensembl genome, v. 109. Because a *D. rerio* ortholog was either not available or returned a one-to-many mapping, untargeted homology and protein domain architecture searches were performed (Table 2). Of these, the most DE genes in the medulla were ENSDLAG00005005740 ($\log_2$FC 6.83) and ENSDLAG00005029440 ($\log_2$FC 5.6), both encoding for complement component C1q domain-containing proteins at their C-terminal regions, usually expressed in collagen-producing cells; ENSDLAG00005024330 ($\log_2$FC 4.98), encoding for a protein containing a C-type lectin-like likely involved in calcium-dependent carbohydrate binding for antigen uptake, cell adhesion, extracellular matrix (ECM) degradation, T cell co-stimulation or homing, depending on domain subgroups based on the presence of additional non-lectin domains and gene structure, as well as cell localization [62]; ENSDLAG00005029446 ($\log_2$FC 3.15), encoding for the membrane-bound form of the CD83 glycoprotein, a recognized marker of human mature DCs [63], where it regulates the expression of cell-surface MHC class II and, in turn, $CD4^+$ T cell development [64]; and ENSDLAG00005012265 ($\log_2$FC 2.78), encoding for antigen WC1.1, a transmembrane glycoprotein belonging to the scavenger receptor cysteine-rich family that is uniquely expressed on γδ T cells involved in proliferation and IFN-gamma production following the binding to autologous antigens [65]. Among the genes whose DE status in the cortex was supported by strongest significance, in addition to the well characterized *rag-1* ($\log_2$FC −4.61), *rag-2* ($\log_2$FC −3.86), *ctsla* ($\log_2$FC −2.80) and *ccl25a* ($\log_2$FC −2.62), were ENSDLAG00005010968 ($\log_2$FC −4.75), encoding for a purpurin-like protein containing a lipocalin/cytosolic fatty-acid binding domain that is usually involved in the binding of a vast array of small hydrophobic ligands, receptor-mediated endocytosis and macromolecular complexation [66,67]: purpurins, in particular, possess both cell-cell and cell-substratum adhesion functions through interaction with specific membrane

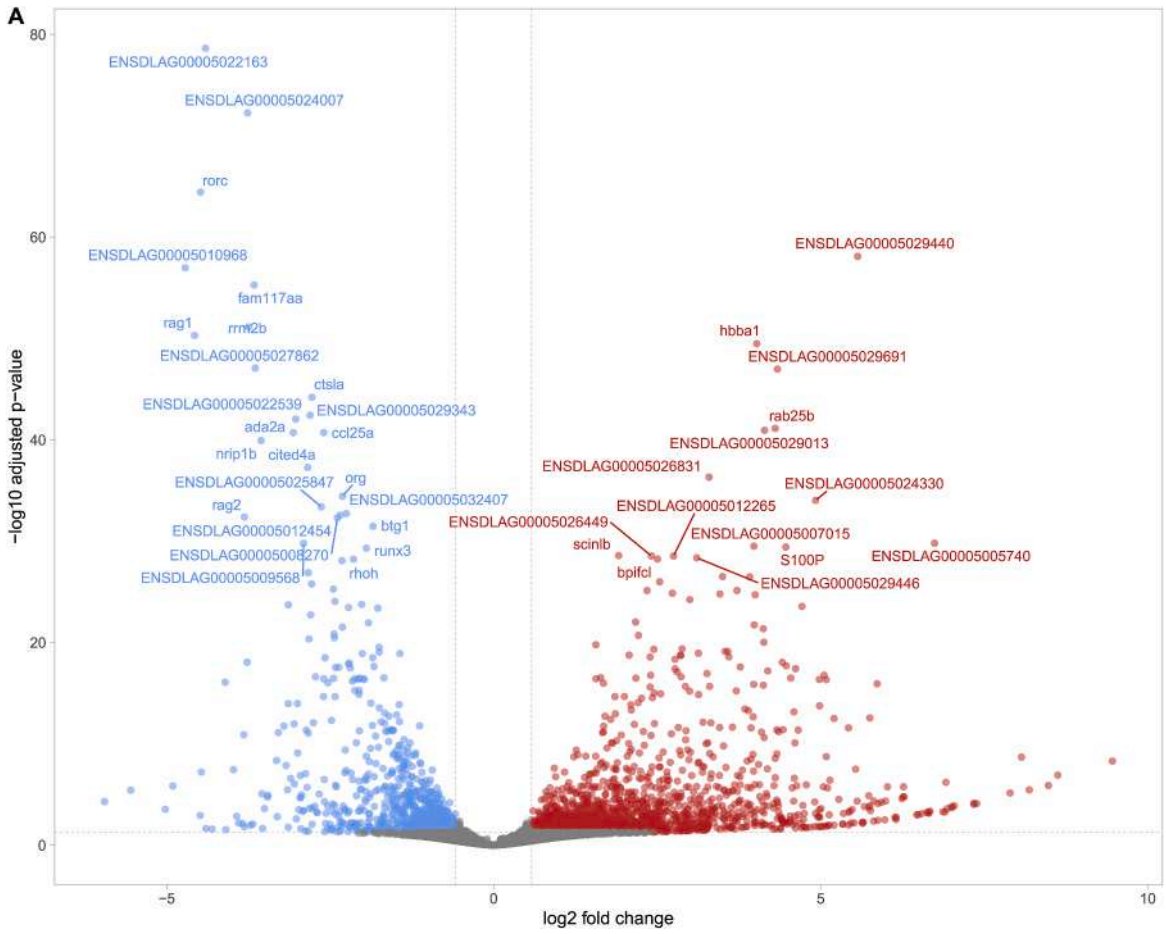

Fig. 2. A) Volcano plot (log_{10} transformed adjusted p-values over shrunk log_2 fold change) of all genes tested for differential expression. Coloring applied when adjusted p-value <0.05 and absolute value of log_2 fold change greater than 0.58 (i.e. fold change = 1.5). The top 40 genes showing strongest statistical support as to their differential expression (i.e. lowest adjusted p-value) between thymic regions are labeled by ZFIN gene name or Ensembl gene ID (if gene name was not available). B) Heatmap and hierarchical clustering of the counts of the top 40 genes whose differentially expressed status between thymic regions was associated with strongest statistical support. Gene labels by ZFIN gene name or Ensembl gene ID (if gene name was not available). Log_2 fold change estimates from DESeq2 results are reported next to gene labels. Expression counts were normalized with the median-of-ratios method of the DESeq2 package and Z-score-scaled on a gene-by-gene basis (i.e. counts were removed of the mean and divided by standard deviation across biological replicates). Columns indicate biological replicates.

receptors [68] as well as cell differentiation and survival roles [69]; ENSDLAG00005022163 (log_2FC −4.43), encoding for the transcriptional repressor zinc finger protein Gfi-1b-like that positively impacts the differentiation of granulocyte and monocyte progenitor (i.e. DCs and macrophages) as well as common lymphoid progenitor (i.e. T cells) [70]; ENSDLAG00005024007 (log_2FC −3.78), encoding for the artemis protein, which is recruited and phosphorylated by DNA-dependent protein kinases for opening hairpin structures at coding ends prior to DNA repair of the rag-1/2-generated DNA double-strand breaks and whose metallo-beta-lactamase domain constitutes the minimal core catalytic domain needed for V(D)J recombination [71,72]; ENSDLAG00005009568 (log_2FC −2.94), encoding for psmb11, a proteolytic subunit of the thymoproteasome exclusively and constitutively expressed by cortical thymic epithelial cells (cTECs) that is essential for optimal positive selection of $CD8^+$ T cells [73] but which also appears to affect the maturation of $CD4^+$ T cell repertoire via gene expression regulation in cTECs [74].

Overall, log_2 fold change distribution per effect size direction is shown in Table S2. The complete lists of differentially expressed genes and of all genes tested for statistical significance are available in Tables S1A and S1B, respectively. Punctiform validation of gene expression conducted by qPCR assays confirmed the DESeq2 transcriptional regionalization of all selected markers (*rag-1*, *TCRβ* and *CD4* over-expressed in the cortex, and *CD83* over-expressed in the medulla), pointing to the reliability of the DEG analysis (Figs. S1A–B).

3.4. Transcriptional localization of thymic markers of lymphoid and non-lymphocytic cells

By combining targeted transcriptome mining using both local *blastp* and *blastx* against custom-built and NCBI non-redundant protein sequences database with protein domain and feature searches, 25 immune-related genes, uncharacterized in the Ensembl database and for which an annotation was not available on *biomaRt*, were identified (Table S3). The differential transcriptional signatures of select thymic markers belonging to lymphoid and non-lymphocytic (i.e. thymic epithelial cells) cells, including those annotated in-house as above, were then extracted and the rationale for including them into the table justified with recent literature of the field published on human, mouse and teleost models (Table 3).

3.5. Functional analyses of thymic transcriptome

3.5.1. Over-representation analysis

A one-to-one zebrafish orthologous gene mapping was retrieved and converted to Entrez IDs, resulting in a working dataset of 9827 unique

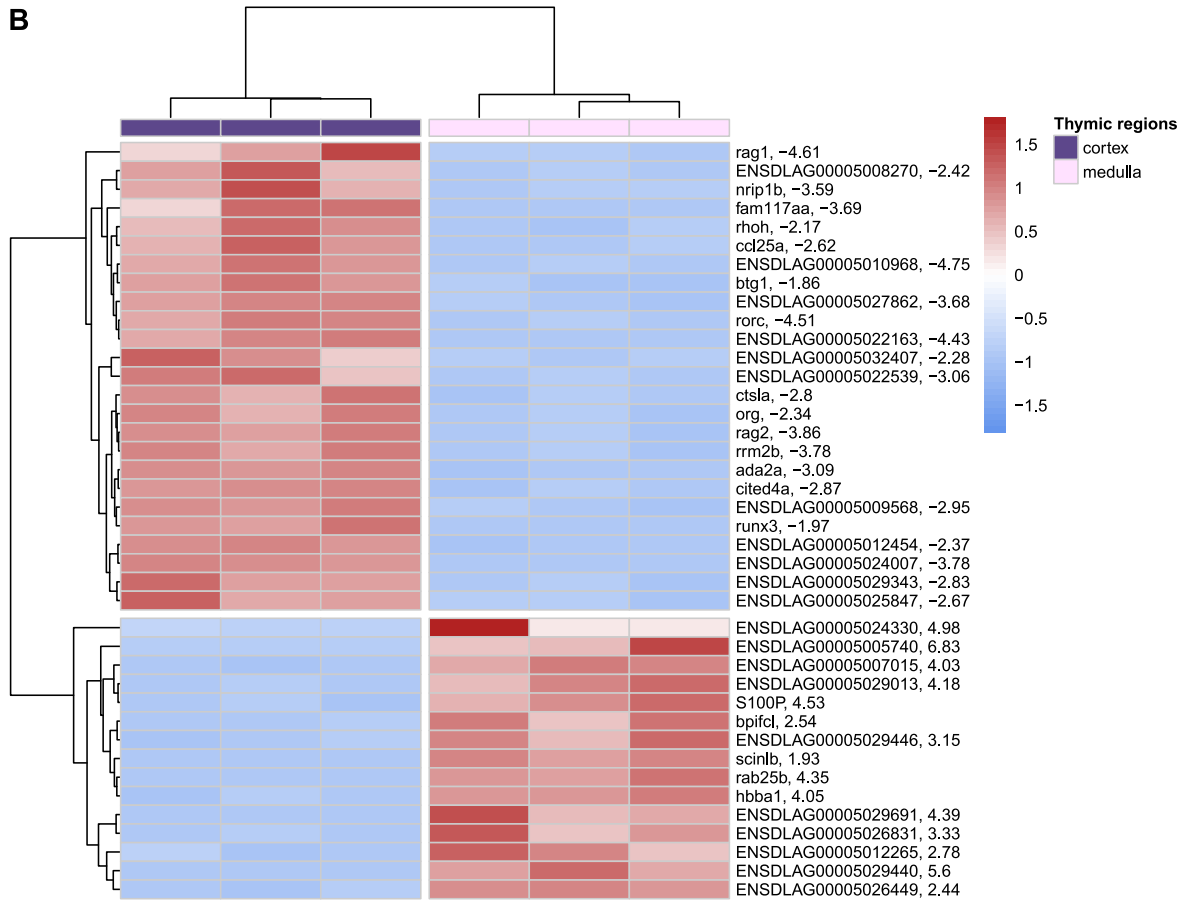

Fig. 2. (*continued*).

genes, including 1638 (937 and 701 over- and under-expressed) DE genes.

An over-representation analysis of Gene Ontology terms was conducted to gain greater biological insight on the differentially expressed genes. One hundred thirty-three (94 biological processes -BP-, 14 cellular components –CC– and 25 molecular functions -MF-) statistically enriched terms were found when testing all DEGs regardless of the $\log_2$ fold change direction (Table S4A). Two hundred fifty-eight (197 BP, 26 CC, 35 MF) and 35 (28 BP, 4 CC, 3 MF) resulted as statistically enriched when testing over-expressed (Fig. 3A, Table S4B) and under-expressed DEGs (Fig. 3B, Table S4C).

"Immune response", "Response to external stimulus", "Leukocyte activation", "Cell adhesion", "Chemotaxis", "Inflammatory response", "G protein-coupled receptor signaling pathway" and "Leukocyte migration" were among the statistically enriched BP terms associated with DE genes over-expressed in the medulla; "Extracellular region", "Intermediate filament", "Extracellular matrix", "Cell surface" and "Cell-substrate junction" were the most impacted cellular components; signaling receptor, molecular transducer, cytokine receptor, immune receptor and peptidase activities were among the most enriched molecular functions: these results overall confirm that a profound cytoskeleton and cell-substrate re-organization, together with transmembrane signaling receptor-driven cell activation, occur in the medulla of the European sea bass (Table S4B).

Genes with a statistically greater expression in the cortex than in the medulla were instead associated with "Histone modification", "Chromatin organization", "Negative regulation of DNA-templated transcription" and "Mitotic cell cycle" biological processes: taking into account the enriched cell compartments and molecular activities, the greater extent of histone, chromatin and protein binding activities in the cortical zone of the thymus is highlighted (Table S4C). Worthy of note is the evidence of epithelial cell migration, as regulated by e.g. fibroblast growth factor 16 (*fgf16*), annexin 1a (*anxa1a*), zeta chain of T cell receptor associated protein kinase 70 (*zap70*), *cd40* and delta-like canonical Notch ligand 4 (*dll4*), as well as the positive regulation of apoptotic process regulated by e.g. dual specificity phosphatase 6 (*dusp6*), cathepsins K, S and L (*ctsk*, *ctss1* and *ctsl.1*), serine/threonine kinase 17b (apoptosis-inducing) (*stk17b*) and pro-apoptotic WT1 regulator (*pawr*), only resulting from the global and over-expressed over-representation tests exploiting the better curated *D. rerio* annotation of orthologous genes (Tables S4A–B).

The validity of such a bioinformatic workflow employing gene ontologies, gene sets and pathways annotations of zebrafish was previously assessed by running an over representation analysis of Gene Ontology (GO) terms on DEGs using *D. labrax* Ensembl ID as gene nomenclature (i.e. no gene ID conversion required). An overlap of GO terms was found between the two datasets (e.g. "Immune response", "Inflammatory response", "Chemotaxis", "G protein-coupled receptor signaling pathway" and nucleosome- and chromatin-related terms) (Tables S5A–C), allowing for the use of better curated and more readily available zebrafish annotations for downstream more detailed functional analysis.

3.5.2. Gene Set Enrichment Analysis

A GSEA was conducted to verify whether coordinated changes in gene expression data occur in the two thymic zones based on *a priori* defined molecular pathways.

The GSEA analysis of KEGG pathways identified 10 statistically-modulated gene sets (Fig. 4A, Table S6A): "Carbon metabolism", "Toll-like receptor signaling pathway", "Glycolysis/Gluconeogenesis"

Table 2
Homology and protein domain architecture characterization of the 21 out of 40 unannotated DEGs supported by strongest statistical support. "gene": gene Ensembl ID; "acc": NCBI accession ID of the first *blastx* hit sorted by highest alignment score, i.e. score calculated from the sum of the rewards for matched amino acids and penalties for mismatches and gaps; "per.id": percent identity of the alignment; "domain": functional and/or structural protein architecture accession ID as per SMART (e.g. SM00409), Pfam (e.g. PF00129) or PDB (e.g. 3PG6|D) databases.

gene	best hit	acc	e-value	per. id	domain	domain name
ENSDLAG00005022163	zinc finger protein Gfi-1b-like [*Dicentrarchus labrax*]	XP_051244740.1	0.00E+00	99	SM00355	ZnF_C2H2
ENSDLAG00005024007	protein artemis [*Dicentrarchus labrax*]	XP_051248246.1	0.00E+00	100	PF07522	DNA repair metallo-beta-lactamase
ENSDLAG00005029440	complement C1q-like protein 4 [*Dicentrarchus labrax*]	XP_051257823.1	5.00E-79	100	SM00110	C1Q
ENSDLAG00005027862	histone H2A-like [*Carcharodon carcharias*]	XP_041037812.1	4.00E-62	100	SM00414	H2A
ENSDLAG00005010968	purpurin-like [*Dicentrarchus labrax*]	XP_051278957.1	5.00E-142	100	PF00061	Lipocalin/cytosolic fatty-acid binding protein family
ENSDLAG00005029691	lysozyme g isoform X2 [*Dicentrarchus labrax*]	XP_051240211.1	2.00E-136	100	PF01464	Transglycosylase SLT domain
ENSDLAG00005029343	uncharacterized protein si:busm1-163l24.3 [*Dicentrarchus labrax*]	XP_051244322.1	0.00E+00	100	PF07292,3PG6|D	Nmi/IFP 35 domain, ligase
ENSDLAG00005022539	equilibrative nucleoside transporter 1 [*Dicentrarchus labrax*]	XP_051275947.1	0.00E+00	100	PF01733	Nucleoside transporter
ENSDLAG00005029013	hemoglobin subunit alpha-A [*Dicentrarchus labrax*]	XP_051245327.1	7.00E-99	100	PF00042	Globin
ENSDLAG00005026831	zinc finger and BTB domain-containing protein 7B isoform X1 [*Dicentrarchus labrax*]	XP_051261420.1	0.00E+00	100	SM00225, SM00355	BTB,ZnF_C2H2
ENSDLAG00005024330	galactose-specific lectin nattectin-like [*Dicentrarchus labrax*]	XP_051281755.1	1.00E-90	89.09	SM00034	CLECT
ENSDLAG00005025847	inosine-uridine preferring nucleoside hydrolase-like [*Dicentrarchus labrax*]	XP_051283665.1	0.00E+00	100	PF01156	Inosine-uridine preferring nucleoside hydrolase
ENSDLAG00005032407	STING ER exit protein [*Dicentrarchus labrax*]	XP_051237040.1	2.00E-136	100	NA	NA
ENSDLAG00005012454	lysosome membrane protein 2 isoform X1 [*Dicentrarchus labrax*]	XP_051268495.1	0.00E+00	100	PF01130	CD36 domain
ENSDLAG00005008270	PRELI domain-containing protein 1, mitochondrial [*Dicentrarchus labrax*]	XP_051239780.1	6.00E-142	100	PF04707	PRELI-like family
ENSDLAG00005005740	complement C1q-like protein 4 [*Dicentrarchus labrax*]	XP_051257824.1	2.00E-90	100	SM00110	C1Q
ENSDLAG00005009568	proteasome subunit beta type-11-like [*Dicentrarchus labrax*]	XP_051232093.1	0.00E+00	100	PF00227	Proteasome subunit
ENSDLAG00005007015	alpha-elapitoxin-As2a-like [*Morone saxatilis*]	XP_035537337.1	3.00E-69	91.6	PF00021	u-PAR/Ly-6 domain
ENSDLAG00005026449	uncharacterized protein LOC118337072 isoform X1 [*Morone saxatilis*]	XP_035529809.1	0.00E+00	95.19	SM001490	DDE_Tnp_4 domain
ENSDLAG00005012265	antigen WC1.1 [*Dicentrarchus labrax*]	XP_051281293.1	0.00E+00	100	PF00530	Scavenger receptor cysteine-rich domain
ENSDLAG00005029446	CD83 antigen [*Dicentrarchus labrax*]	XP_051261376.1	2.00E-147	100	SM00409	IG domain

and "Biosynthesis of amino acids" were associated to a positive Normalized Enrichment Score (NES) ranging from 1.71 to 1.80 and associated to the medullary environment, while "Non-homologous end-joining", "Nucleotide metabolism", "Proteasome", "FoxO signaling pathway", "Cell cycle" and "Autophagy - animal" had a negative NES ranging from −1.82 to −1.65 and were therefore associated to the cortical environment. We remind that a positive score indicates gene set enrichment at the top of the ranked list, while a negative one indicates gene set enrichment at the bottom of the ranked list, where the ranking metric was calculated as a function of the $\log_2$ fold change sign multiplied by the log-transformed Wald test p-value. The greatest percentage of genes included in the leading edge subset, and therefore contributing the most to the enrichment score, was 16 % (positive NES) and 13 % (negative NES). The complete list of modulated KEGG gene sets returned by not setting any significance cut-off is available as Table S6B, while selected enriched KEGG pathways annotated with $\log_2$ fold change estimates are available in Figs. S2A–G.

The same GSE analysis performed on REACTOME pathways also identified 10 statistically modulated gene sets (Fig. 4B, Table S7A). "Innate Immune System", "GPCR downstream signaling", "Degradation of the extracellular matrix" and "Extracellular matrix organization" were associated with positive NESs ranging from 1.58 to 1.86. "Chromatin modifying enzymes", "Chromatin organization", "DNA Repair", "Nonhomologous End-Joining (NHEJ)", "RNA Polymerase II Transcription" and "Gene expression (Transcription)" instead were associated to negative NESs ranging from −1.88 to −1.57. "GPCR downstream signaling" and "Gene expression (Transcription)" were the two gene sets that comprised the greatest number of genes (19 % and 18 %, respectively) contributing the most to the enrichment score. The complete list of modulated Reactome gene sets returned by not setting any significance cut-off is available as Table S7B.

The complex cross-talk across core enrichment genes (i.e. genes that contributed the most to the enrichment scores reported above) and biological concepts for each of the statistically enriched pathways of both databases are shown in gene linkage mode in Fig. 5A–B. Attention is called upon the relationship between the autophagic process and the FoxO signaling pathway (*gabarapl2* - GABA type A receptor associated protein like 2 - and *zgc:55558* - a RAS-superfamily GTPase) (Fig. 5A), the innate immune system and the degradation/organization of the extracellular matrix (*ctsba* - cathepsin B - and *adam8a* -disintegrin and metalloprotease domain 8) (Fig. 5B), as well as on the clustered spatial allocation of the gene sets with regards to thymic zonation and transcriptional signatures, providing evidence for the distinct cytological and biological features of thymic regions in the European sea bass.

3.5.3. Signaling pathway impact analysis

To overcome the limitations of both over-representation analysis and functional class scoring techniques consisting in the independent

Table 3
Transcriptional patterns of select differentially-expressed thymic biomarkers, sorted in ascending order according to $\log_2$ fold change estimate (i.e. first over-expressed in the cortex, then in the medulla). padj: Benjamini-Hochberg adjusted p-value, FDR cut-off of 0.05; name: gene name annotation provided by the biomaRt R package; description: gene description provided by the biomaRt R package (i.e. "[Source: ZFIN …]") or resulting from the best hit of *blastx* searches against the NCBI non-redundant protein sequences database.

gene	log2FoldChange	padj	name	description	role
ENSDLAG00005009323	−4.612327074	4.85284E-51	rag1	recombination activating gene 1 [Source:NCBI gene;Acc:30663]	Direction of V, D, and J segments recombination for random generation of T cell receptors.
ENSDLAG00005009319	−3.859251079	4.04924E-33	rag2	recombination activating gene 2 [Source:NCBI gene;Acc:30658]	Direction of V, D, and J segments recombination for random generation of T cell receptors.
ENSDLAG00005009568	−2.945056651	1.64865E-30	ENSDLAG00005009568	proteasome subunit beta type-11-like [*Dicentrarchus labrax*]	Proteasomal subunit (β5t) of the thymoproteosome exclusively present in cTEC. Essential for production of the unique peptide motifs required for positive selection of $CD8^+$ T cells. Promotes cortex-to-medulla migration of developing thymocytes.
ENSDLAG00005020923	−2.877628004	1.23998E-27	ENSDLAG00005020923	thymus-specific serine protease isoform X2 [*Dicentrarchus labrax*]	Involved in the positive selection of CD4 T cells. Marker of cTEC lineage.
ENSDLAG00005022121	−2.803072939	6.18388E-45	ctsla	cathepsin La [Source:ZFIN;Acc:ZDB-GENE-030131-106]	Involved in the positive selection of CD4 T cells. Marker of cTEC lineage.
ENSDLAG00005023367	−2.63133109	3.11131E-19	ENSDLAG00005023367	M1-specific T cell receptor beta chain-like [*Thunnus maccoyii*]	TCR^+ cells are positively selected in the cortex based on TCR engagement with MHC molecules. TCRβ expression alone triggers expression of CD4 and CD8 coreceptors as well as TCRα gene rearrangement.
ENSDLAG00005011442	−2.623985117	1.88427E-41	ccl25a	chemokine (C–C motif) ligand 25a [Source:ZFIN;Acc:ZDB-GENE-110222-1]	Chemotactic activity for dendritic cells, thymocytes, and activated macrophages in mammals and seems responsible for thymus homing in fish. Originally described as thymus-expressed chemokine or TECK. Potential marker of cTEC. Ligand of CCR9.
ENSDLAG00005014934	−2.419821564	0.030988751	ly75	lymphocyte antigen 75 [Source:ZFIN;Acc:ZDB-GENE-050309-166]	Also known as CD205. Type I transmembrane protein mediating absorptive endocytosis of extracellular glycoprotein antigens for antigen processing and presentation. Marker of cTEC lineage.
ENSDLAG00005005402	−2.25373708	3.40026E-24	cd4-1	CD4-1 molecule [Source:ZFIN;Acc:ZDB-GENE-100922-280]	Co-receptor of T cells belonging to the immunoglobulin superfamily. $CD4^+$ T lymphocytes are functionally similar to mammalian helper T cells (Th).
ENSDLAG00005001682	−1.781054754	2.98195E-20	ENSDLAG00005001682	T-cell surface glycoprotein CD3 delta chain [*Dicentrarchus labrax*]	Complexed with αβ or γδ TCR heterodimers, CD3 co-receptors play essential roles in specific antigen recognition, cell activation and signal transmission in T cells. Belongs to the immunoglobulin superfamily. Master T cell surface marker.
ENSDLAG00005030987	−1.644562244	0.000153731	ENSDLAG00005030987	T-cell receptor gamma chain precursor [*Dicentrarchus labrax*]	Part of the γδ TCR heterodimer that is expressed by T cells proposed as a primordial lymphocyte population predating αβ T cells and B cells, and accordingly located at the interface between innate and acquired immunities.
ENSDLAG00005001518	−1.622564208	0.00505339	dll4	delta-like 4 (*Drosophila*) [Source:ZFIN;Acc:ZDB-GENE-041014-73]	Induces Notch signaling in thymic immigrant cells and is therefore indispensably required by the thymus-specific environment for T cell fate determination. Interference with dll4a expression diminishes the T cell receptor beta chain expression in thymocytes and leads to disappearance of CD4 CD8 double-positive or single-positive T cells.
ENSDLAG00005018027	−1.476003208	1.29968E-14	ENSDLAG00005018027	C–C chemokine receptor type 9 [*Dicentrarchus labrax*]	Receptor of ccl25a. Regulates thymus homing (migratory behavior) of developing T cells. Potential marker for thymocytes undergoing negative selection, which interact with dendritic cells.
ENSDLAG00005006795	−1.423072959	1.22048E-08	ENSDLAG00005006795	T cell receptor alpha chain, partial [*Dicentrarchus labrax*]	TCR^+ cells are positively selected in the cortex based on TCR engagement with MHC molecules.
ENSDLAG00005001701	−1.366414294	0.001682884	ENSDLAG00005001701	T-cell surface glycoprotein CD3 epsilon chain [*Dicentrarchus labrax*]	Complexed with αβ or γδ TCR heterodimers, CD3 co-receptors play essential roles in specific antigen recognition, cell activation and signal transmission in T cells. Belongs to the immunoglobulin superfamily. Master T cell surface marker.
ENSDLAG00005012726	−1.199368362	4.8913E-06	zap70	zeta chain of T cell receptor associated protein kinase 70 [Source:ZFIN;Acc:ZDB-GENE-050522-257]	Tyrosine kinase protein (70 kDa). It is expressed near the surface membrane of T cells and recruited upon antigen binding to the TCR, where it initiates a signal pathway downstream. Crucial for selective activation of T cells.

(*continued on next page*)

Table 3 (*continued*)

gene	log2FoldChange	padj	name	description	role
ENSDLAG00005010631	0.949338543	2.46242E-08	krt5	keratin 5 [Source:ZFIN;Acc:ZDB-GENE-991110-23]	Marker of mTEC lineage.
ENSDLAG00005027038	1.067295466	0.00035589	cd40	CD40 molecule, TNF receptor superfamily member 5 [Source:ZFIN;Acc:ZDB-GENE-090313-95]	Type I membrane-bound protein, member of TNF receptor family, receptor of CD40L. Contributes to controlling differentiation of mTEC from thymic epithelial progenitors. Regulates expression of Aire (autoimmune regulator).
ENSDLAG00005011637	1.116395667	5.95994E-08	ENSDLAG00005011637	MHC class II antigen beta chain [*Dicentrarchus labrax*]	Membrane-bound glycoproteins binding antigenic determinants. Expressed on mTECs, MHCs present the peptides of tissue-restricted antigen (TRA): $CD4^+$ T cells recognizing self-antigens are eliminated by apoptosis (negative selection) or differentiate into regulatory T cells (agonist selection)
ENSDLAG00005028731	1.125218388	2.85448E-05	ENSDLAG00005028731	H-2 class I histocompatibility antigen, Q9 alpha chain isoform X7 [*Dicentrarchus labrax*]	Part of MHC class I displaying peptide fragments of proteins to $CD8^+$ T cells.
ENSDLAG00005003259	1.593901754	0.00337377	ENSDLAG00005003259	T-lymphocyte activation antigen CD80 isoform X1 [*Dicentrarchus labrax*]	Involved in activation and differentiation of $CD4^+$ T cells, it binds CD28 following the first interaction between TCR and peptide-MHCII complex. It also binds CTLA-4. Marker of mTEC lineage.
ENSDLAG00005027937	1.826164504	0.005859493	cxcr3.2	chemokine (C-X-C motif) receptor 3, tandem duplicate 2 [Source:NCBI gene;Acc:791973]	Enables C–C chemokine binding activity and C–C chemokine receptor activity. Acts within chemokine-mediated signaling pathway, leukocyte migration and macrophage activation involved in immune response.
ENSDLAG00005017672	1.875996152	8.39193E-11	ENSDLAG00005017672	T-cell-specific surface glycoprotein CD28 [*Dicentrarchus labrax*]	T cell co-receptor. Surface-associated molecules involved in the activation, proliferation and differentiation of T cells by coordinating the secondary. Ligand of CD80.
ENSDLAG00005008193	1.88438138	0.0253678	csf1ra	colony stimulating factor 1 receptor, a [Source:NCBI gene;Acc:64274]	Growth factor receptor of mammalian dendritic cells (DCs). Typically associated to DC function and antigen presentation, together with il12 and MHC class II invariant chain iclp1.
ENSDLAG00005006077	1.968993288	0.021771429	krt18b	keratin 18b [Source:ZFIN;Acc:ZDB-GENE-040426-1508]	Type I keratin commonly expressed by epithelial cells. Maintains mechanical stability and integrity of epithelial cells, and, as caspase substrate, is also involved in regulating intracellular cell-death signaling pathways.
ENSDLAG00005021633	2.361482832	5.93318E-12	CXCR4	C-X-C motif chemokine receptor 4 [Source:HGNC Symbol;Acc:HGNC:2561]	Receptor of CXC chemokine ligand 12 (CXCL12). Member of seven-transmembrane (7-TM) G-protein-coupled receptor superfamily. Together with Ccr9/Ccl25, the cooperative activity of the Cxcr4/Cxcl12 pair regulate thymus homing by chemotactic activity.
ENSDLAG00005031878	2.446213096	2.40978E-16	cd40lg	CD40 ligand [Source:ZFIN;Acc:ZDB-GENE-100727-1]	39-kDa glycoprotein of the TNF family found on activated $CD4^+$ T cells. CD40L-CD40 interactions direct T lymphocyte maturation towards the Th1 phenotype through the induction of proinflammatory cytokines in mammls. CD40L-CD40 contributes to maintaining functional communication between T lymphocytes and DCs.
ENSDLAG00005025962	2.978082054	0.007567078	ccl25b	chemokine (C–C motif) ligand 25b [Source:ZFIN;Acc:ZDB-GENE-110222-2]	Previously known as ccl21. Highly expressed by mTECs. Ligand of CCR7.
ENSDLAG00005013506	3.001865635	2.10691E-16	foxp3b	forkhead box P3b [Source:ZFIN;Acc:ZDB-GENE-081104-332]	Transcription factor characteristically expressed in T reg cells, where it regulates the transcription of genes related to establishing the T reg lineage and T cell activation. $Foxp3^+$ Treg cells are mainly distributed in the thymic medulla and migrate to peripheral tissues.
ENSDLAG00005029446	3.146471246	4.29463E-29	ENSDLAG00005029446	CD83 antigen [*Dicentrarchus labrax*]	Glycoprotein, member of the Ig superfamily. Suggested autocrine immune regulation by interaction between membrane bound and soluble forms. Soluble form produced in large amounts by activated Treg cells. Established role in peripheral Treg cell induction. Involved in $CD4^+$ thymocyte maturation. Marker of mature DCs, where it stabilizes MHC II.
ENSDLAG00005031923	3.653007606	7.46469E-20	zbtb16a	zinc finger and BTB domain containing 16a [Source:NCBI gene;Acc:323269]	Gene encoding for promyelocytic leukemia zinc finger, a member of the BTP/POZZF family of transcription factors. Early transcriptional regulator for commitment of natural killer T cell (NKT cell) lineage

(*continued on next page*)

Table 3 (*continued*)

gene	log2FoldChange	padj	name	description	role
ENSDLAG00005006996	4.8988644	2.18603E-06	aire	autoimmune regulator [Source: ZFIN;Acc:ZDB-GENE-071008-4]	Interaction with transcriptional regulators to induce the transcription of self-antigens such as TRAs. Regulates mTEC differentiation and function, for example, mTEC maturation and expression of Ccr7 and Ccr4 ligands.
ENSDLAG00005007992	5.372366696	3.02684E-13	ENSDLAG00005007992	C–C motif chemokine 19-like [*Dicentrarchus labrax*]	Highly expressed by mTECs. Ligand of CCR7.
ENSDLAG00005004098	6.238950956	0.003475562	il12ba	interleukin 12Ba [Source:ZFIN; Acc:ZDB-GENE-050525-3]	Typically associated to DC function and antigen presentation, together with csf1r and MHC class II invariant chain iclp1.

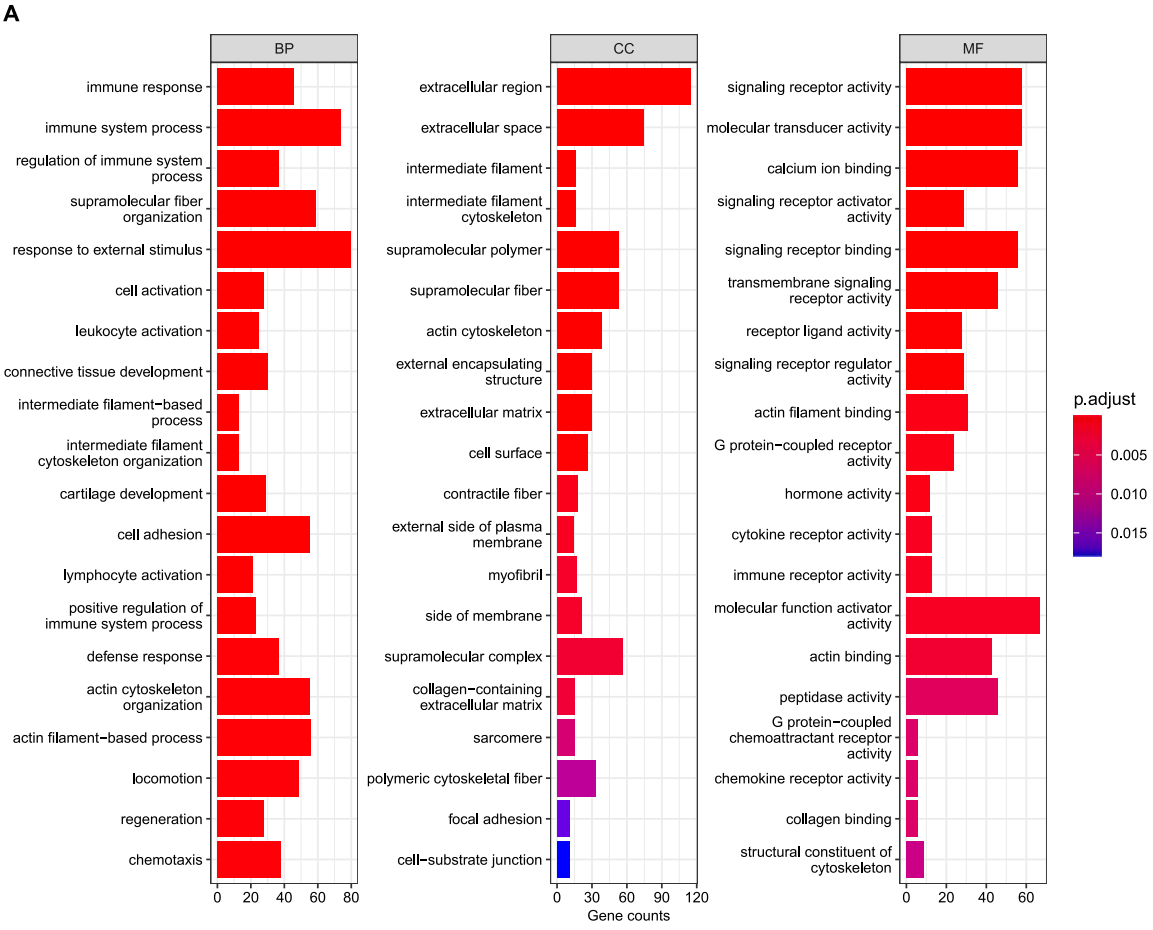

Fig. 3. Barplot of the top 20 (according to q-value) enriched GO terms per ontology associated with A) over-expressed and B) under-expressed orthologous DE genes over gene counts per term. Color coding is based on statistical significance of the over-representation.

analysis of each functional category and the lack of a unifying analysis at the system level [75], a signaling pathway impact analysis incorporating multiple evidence sources, such as log fold-change estimates of DE genes, the statistical significance of the set of genes belonging to a given pathway and the topology of the pathway itself, was conducted to estimate the actual impact of such transcriptional changes between the two thymic regions and, in turn, identify affected pathways.

The KEGG pathways of "Neuroactive ligand-receptor interaction" (4080), "Focal adhesion" (4510), "Cytokine-cytokine receptor interaction" (4060), and "Intestinal immune network for IgA production" (4672) resulted as positively perturbed (i.e. activated) in the medulla (Fig. 6). The first three pathways were identified as statistically significant according to the Bonferroni-corrected global probability value, while the fourth was statistically significant only according to the FDR-corrected global p-value (Table S8). The pathway of "Focal adhesion" was the one comprising the greatest number of total and DE genes, while the activation status of "Neuroactive ligand-receptor interaction" had the strongest statistical support (Table S8).

The pathway of "ECM-receptor interaction" (4512), also activated in the medulla according to a global p-value of 1.07E-2, failed to reach statistical significance with either FDR or Bonferroni corrections (Table S8).

4. Discussion

In all jawed vertebrates, the maturation of T cells occurs in the thymus [14]. Its organization usually agrees with the cortex-medulla mammalian compartmentalization (e.g. Refs. [76,77]), the

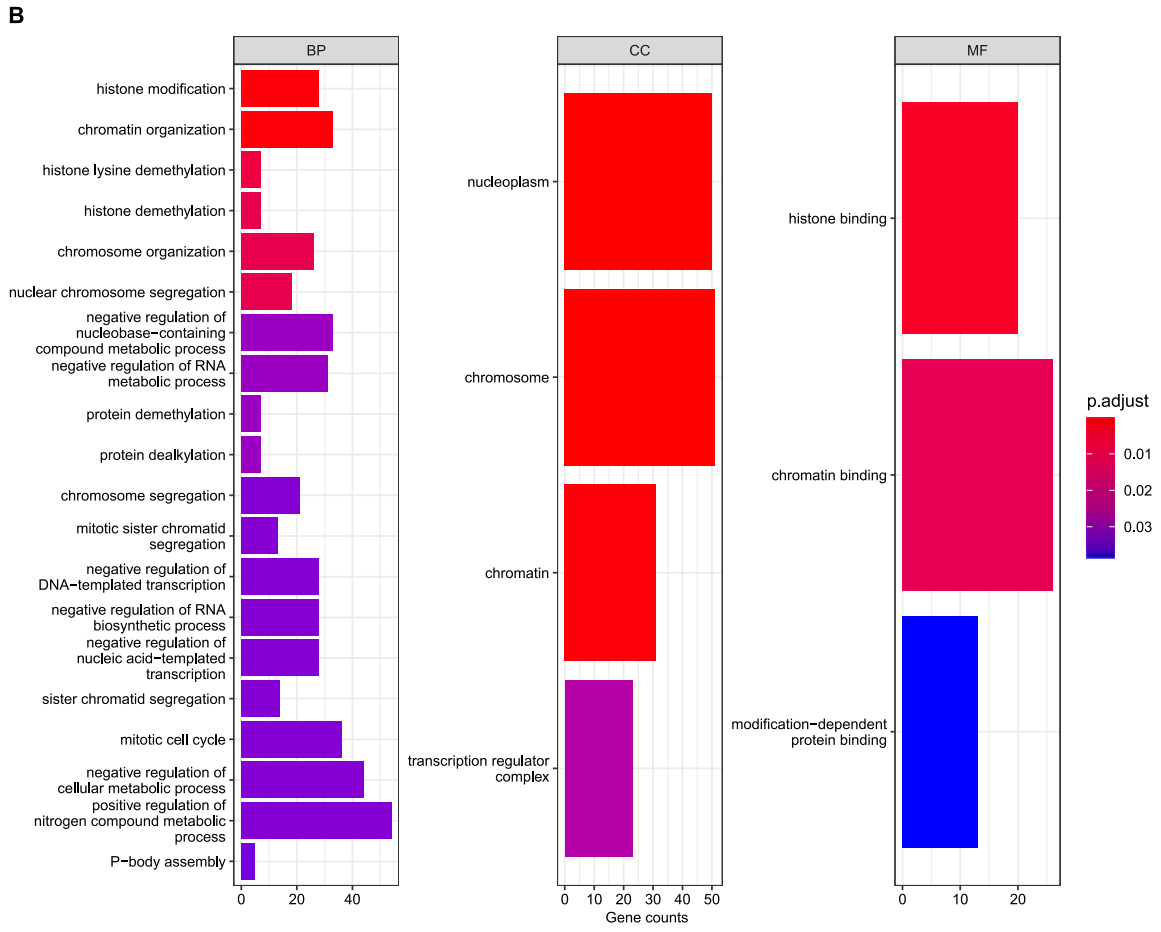

Fig. 3. (*continued*).

architectural, phenotypic and molecular features of which have been thoroughly investigated (e.g. Refs. [78–81]). Despite the interest and efforts devoted to investigating fish adaptive immunobiology, knowledge on teleost thymus remains scarce, and its structural and functional compartmentalization is still one of the open questions.

Most teleosts [17,26], except for few species (e.g. *Paralichthys olivaceus*, *Onchorhynkus mykiss* and *Salmo salar*), display a thymic zonation. In *Dicentrarchus labrax*, a histological distinction between cortex and medulla is clear [29,30] (Fig. 1A–B of this work): the former appears darkly stained due to the higher density of small and immature lymphoid cells and the latter is stained palely due to a lower density of cells dispersed within the connective tissue. Such a feature was also supported by transcript profiles of or using antibodies against typical molecules involved in teleost T cell maturation process, hinting at the distinct functions underlay by the two regions (e.g. Refs. [31,37,38]). Herein, based on histological evidence, we leveraged laser capture microdissection to isolate the two thymic zones by direct microscopic visualization, and conducted a comprehensive transcriptome analysis in the European sea bass. In accordance with future perspectives illustrated by Bjørgen and Koppang [26], who recognized the significance of the environment in which genes are expressed and function for gaining deeper insights into their actions, the overall aim of the work was to shed light on the processes and pathways occurring within the cortical and medullary compartments.

Coupled with the omics approach, laser microdissection proved to be a robust and powerful enrichment tool for high-throughput characterization of specific cellular populations, interrogation of cell type-specific molecular profiles and elucidation of biological features with associated molecular mechanisms. We succeeded in optimizing the working protocol, as demonstrated by the yield of RNA and the comparability of raw reads number and mapping percentage onto the *D. labrax* genome (Table 1). The transcriptome analysis revealed a notable amount of differentially expressed genes (i.e. 18.1 % of the total), namely 1458 and 915 over- and under-expressed in medulla compared to the cortex, respectively (Fig. 2A, Table S2). While the greatest possible soundness of our data was reached with the gene set enrichment and the signaling pathway impact analyses (Figs. 4 and 5, Tables S6A-S7A-S8), the mere interpretation of the top 40 DE genes comprising markers of both lymphoid and non-lymphocytic cells already provides a glimpse of the functional compartmentalization of the thymus (Fig. 2A–B, Table 2).

It is known that a complex thymic microenvironment is a prerequisite for the development of fully functional T cells [82]. The microenvironment of the thymus, for instance, defines the outcome of the hematopoietic progenitor differentiation throughout a complex network of interactions including distinct molecular cues, such as transcription factors (e.g. *foxn1*, *foxn4* and FoxO signaling pathway, Fig. 4A–5A, Fig. S2D), chemokine ligands/receptors and cytokines (e.g. *ccl25a/ccr9*, *cxcl12/cxcr4*, *il2r*, *il12b,* Table 3, Table S3) and highly conserved representatives of the Notch signaling pathway (e.g. *notch1/dll4*, Table 3) that interact in a synergistic, context-dependent and hierarchical manner to orchestrate homing, commitment, intra-thymic trafficking, self-tolerance and egress of thymocytes [83–88].

Foxn1 encodes for a transcription factor that is dispensable for the formation of the thymic anlage during embryonic development [89] and, specifically to this context, is critical for the differentiation and maturation of thymic epithelial progenitors into both cTECs and mTECs [90,91] and for the maintenance of the cortico-medullary organization with aging [92]. Our dataset confirmed the expression of Foxn1 and

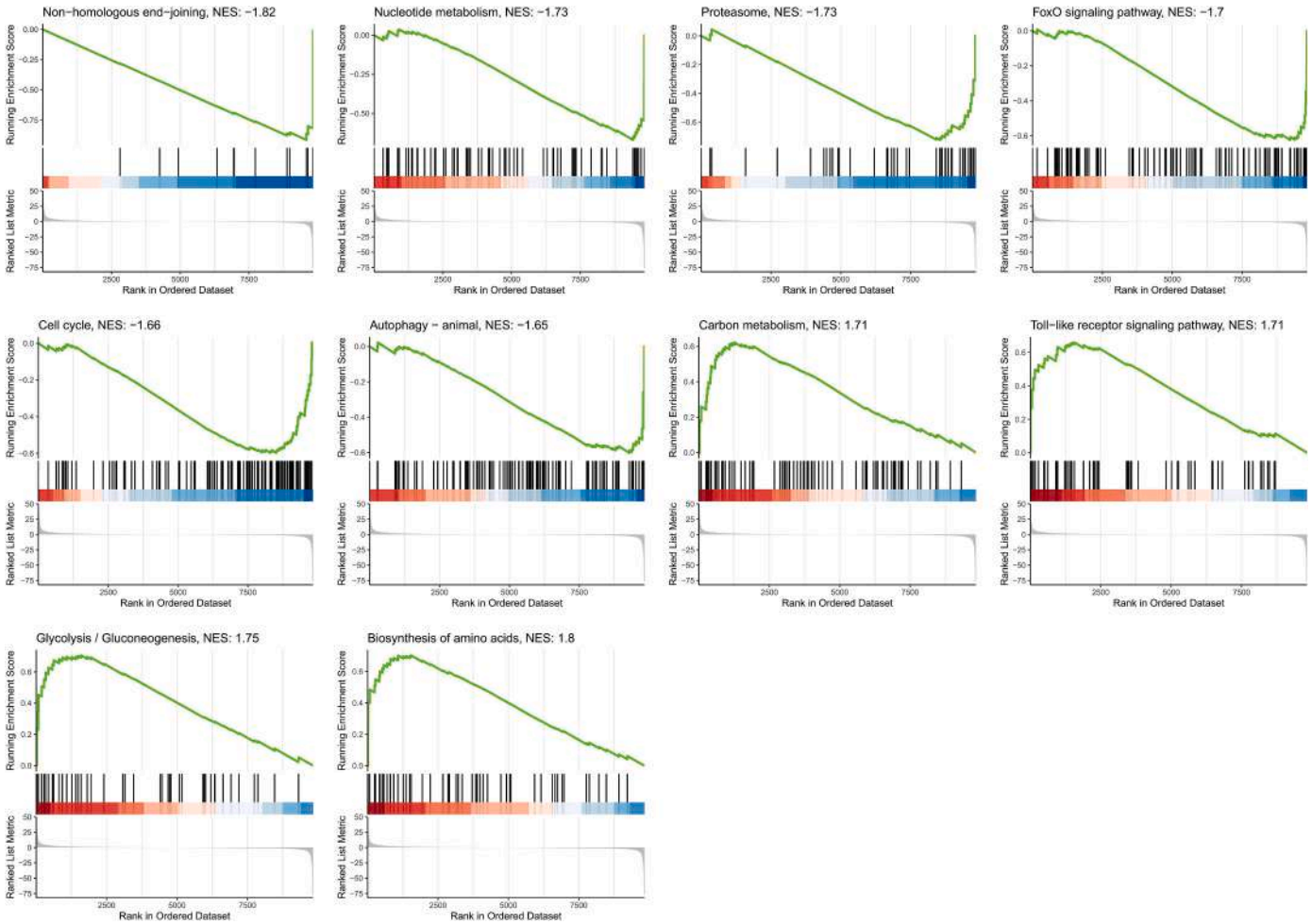

Fig. 4. Gene Set Enrichment Analysis plots of A) KEGG and B) Reactome pathways, sorted by ascending normalized enrichment score (NES), reported next to the pathway title. The profile of the running enrichment score is shown in the top portion of each plot. The middle panel presents the position of gene set members in the rank-ordered list, and the leading-edge subset is evident subsequent or prior to the peak score in case of negative and positive NES, respectively. The bottom portion of each plot reports the value and distribution of the ranking metric.

Foxn4, a Foxn1 paralogous gene; these did not appear to be a unique signature of the cortical microenvironment, as suggested by the lack of statistical support for the higher expressions. While they are known to be co-expressed in TECs [17] and both contribute to thymopoietic activity in teleost species, Foxn1 is both necessary and sufficient in the mammalian thymus [20]. In zebrafish and medaka, Foxn1 directly regulates the expression of *ccl25a* and *dll4*: both of them herein appeared strongly over-expressed in the cortex of sea bass, together with *ccr9*. This information suggests the sea bass cortical microenvironment as the site playing essential roles for homing of lymphoid progenitors [93] and commitment to T-lineage [94].

Somatic recombination was demonstrated to occur in the *D. labrax* cortex through diverse methods and annotation sources (Fig. 2B, 3B, 4A-B, Table 2, Fig. S2C): in particular, *rag-1*, *rag-2* and *artemis* were among the most highly and differentially expressed genes, and chromatin organization, DNA repair, non-homologous end-joining and FoxO signaling pathways were there over-represented or enriched. This is consistent with the progression of a successful V(D)J rearrangement of TCR gene loci, directed by rag-1/2 recombinases, in double-negative (DN, $CD4^{-}CD8^{-}$) cells that had undergone commitment to T-lineage by Notch signals. Rag-1/2 were described in the thymus of several fish species [17], rag-2-expressing cells were localized in the medaka cortex and DN cells were inferred in the outer sea bass cortex [38]. The verification of proper TCR protein expression occurs at the first checkpoint, namely β-selection. Intense proliferative events were herein seen to occur in the cortex by an enrichment of the gene set related to cell cycle (Fig. 4A, Fig. S2E), in agreement with mammalian models: throughout the development of mammalian DNs, thymocytes undergo intense proliferative events before (i.e. from lymphoid progenitors to DN2 stage) and after (i.e. from DN3b to DN4 stages) β-selection [95]: during the latter transition, cell cycling is particularly rapid and governed by complex regulatory metabolism [96]. It is at the DN3 stage that γδ and αβ T cell lineages diverge [97] by engaging distinct metabolic programs [98], and at the DN4 stage that CD8 and CD4 are intensely transcribed and cells differentiate into double positive (DP, $CD4^{+}CD8^{+}$) thymocytes [95,99]. Genes encoding for α, β, γ and δ TCR chains as well as co-receptors CD4, CD8β and the *ε*, δ, and *ζ* CD3 subunits were all identified in, or homology-mined from, the transcriptome (Table 3, Tables S1 and S3); all appeared as over-expressed in the cortex, except for CD8β and TCRδ (for which no expression data was obtained due to a poor 3' UTR annotation) and CD3*ζ* (adjusted p-value of 0.92). Our data also evidenced gene ENSDLAG00005012265 encoding for WC1.1 among the top DE, uniquely expressed on γδ T cells (Table 2).

Also, the second checkpoint of positive selection was confirmed to take place in the sea bass cortex. T cell positive selection occurs thanks to a 3D microenvironment organized by cTECs: they possess unique antigen processing and presentation machineries that broadly consist of autophagy for obtaining proteins that are then processed by either the

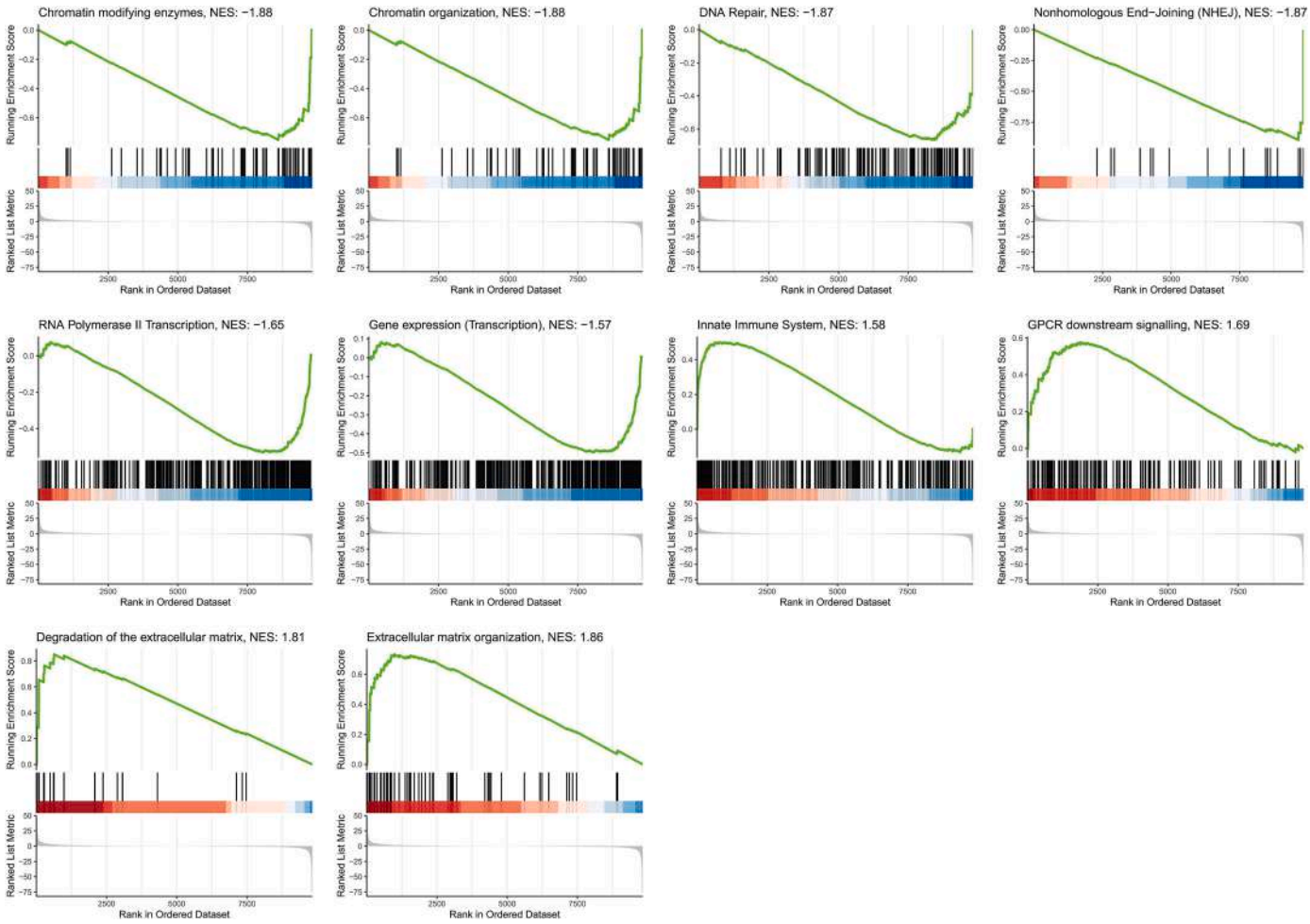

Fig. 4. (*continued*).

thymoproteasome or the proteases cathepsin L and the thymus-specific serine protease (TSSP) [100], and MHCs for self-peptide presentation. All of these signals or gene sets were found either over-expressed, over-represented or enriched in the sea bass cortex (Fig. 2B, 4A and 5A, Tables 2 and 3, Figs. S2B and F, Table S1A).

Autophagy is constitutively active in TECs, and highest activity was detected in mouse cortex, with 60 % of positive cells compared to about 30 % in the medulla [101]. Knowledge in teleost fish is scarce but, for the first time in sea bass, the autophagic process was herein found significantly enriched in the cortex (Fig. 4A, Fig. S2F). Based on mammalian models, this process is confidently involved in T cell positive selection, as one of the non-canonical functions of autophagy is to participate in antigen processing and presentation for the MHC class I and II activation of T lymphocytes [102]. MHCs were previously reported in the cortical region of sea bass (MHC-II) and few other teleosts [37,103,104].

Proteasomes are multi-subunit proteases responsible for the cytoplasmic generation of peptides to be presented by MHC class I. The thymoproteasome is a specific form of the proteasome containing the thymus-specific catalytic subunit β5t, encoded by *psmb11* (proteasome subunit-β type 11), that defines thymic nurse cells (TNCs), a fraction of cTECs [105–107]. The restricted expression of *β5t* in cTECs is a critical factor for thymic selection and maintenance of the peripheral pool of $CD8^+$ T cells [108]. Incorporation of the β5t subunit instead of the constitutive β5 within the 20S enzymatic core reduces the chymotrypsin-like activity of the proteasome, resulting in the generation of a unique set of TCR ligands bound to MHC-I molecules on cTECs with low affinity for promoting positive selection of CD8 SP cells. In this regard, it was recently demonstrated that the thymoproteasome is able to shape the TCR repertoire of $CD8^+$ directly with cortical positive selection independent of apoptosis-mediated negative selection in the medulla [109]. *Psmb11* had a core contribution to the cortical enrichment of the KEGG gene set "Proteasome" in our dataset (Fig. 4A and 5A, Fig. S2B).

Further markers of cTEC were the lysosomal proteases cathepsin L (*ctsla*) and the thymus-specific serine protease (TSSP), also known as *prss16*. Both resulted as DE in the cortex: the former was among the top 40 DE genes (Fig. 2B) and the latter was previously un-annotated in the European sea bass genome (Table S3). Their expression patterns are consistent with literature [110]. Altogether, these data provide the first evidence for the occurrence and mechanistic explanation of positive selection in the sea bass thymic cortex. The ultimate outcome is the selection of T cells displaying functional TCR-MHC interactions for further education in the medulla.

Following positive selection, thymocytes migrate to the thymus medullary region to undergo negative selection against strong TCR-MHC interactions [84], accompanied by dynamic changes in metabolic programs: glycolysis, for instance, is recovered in mature single-positive (SP) stages in murine and human thymus [111]. Our data showed the enrichment of the "Carbon metabolism", "Glycolysis/Gluconeogenesis" and "Biosynthesis of amino acids" gene sets in the sea bass medulla (Fig. 4A, Fig. S2A). These are well-known interconnected processes in cell metabolism as they all involve the utilization and conversion of carbon compounds, particularly carbohydrates, into various biomolecules essential for the cell's growth, energy production, and maintenance.

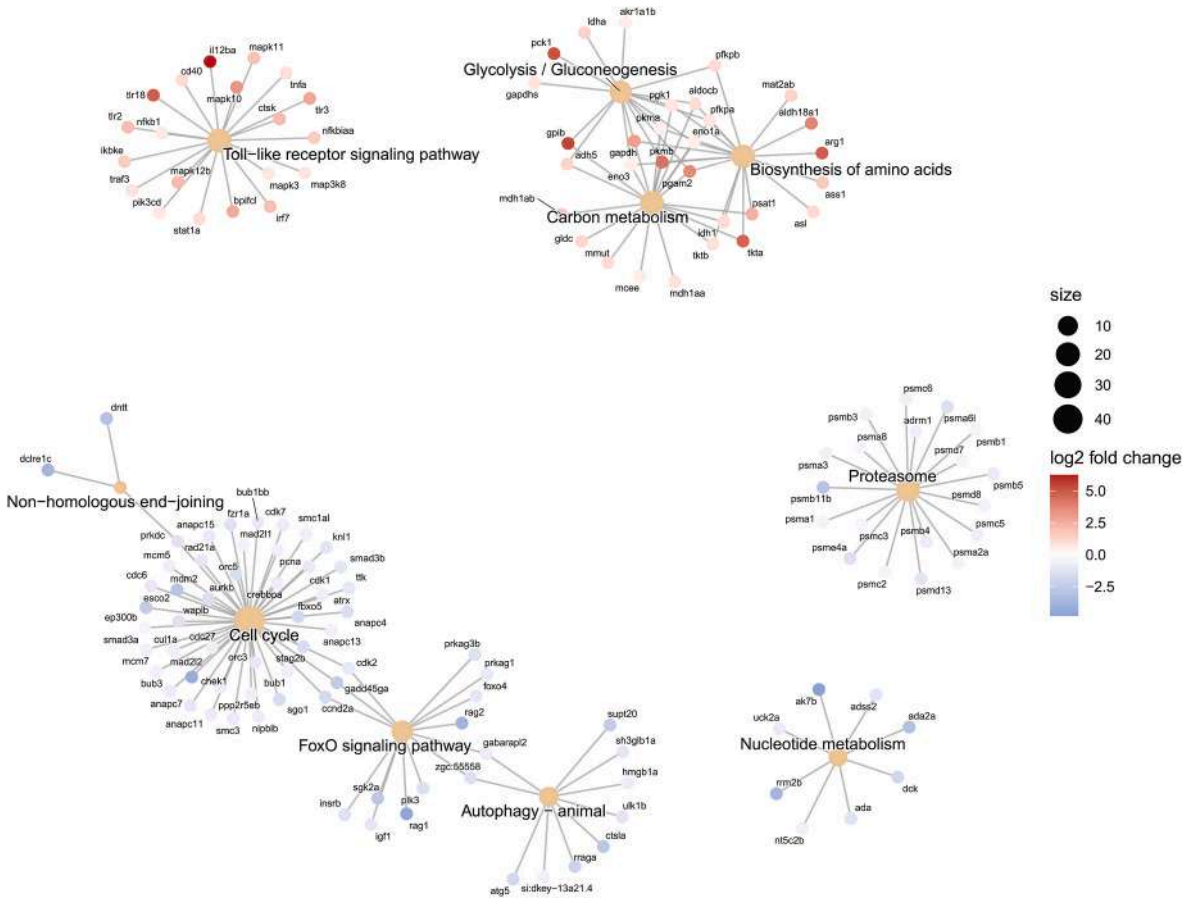

Fig. 5. Effect size-annotated-annotated gene-category network plot depicting the biological complexity and relationships among core enrichment genes of terms identified as significantly enriched by GSEA analysis on A) KEGG and B) Reactome databases. Dot size of categories is proportional to the number of genes.

From our results, the medulla was recognized for its expression of *ccl25b* (log_2FC 2.98, adjusted p-value 7.5E-3) and the autoimmune regulator (*aire*) (log_2FC 4.9, adjusted p-value 2.2E-06) (Table 3) [112, 113], as found in mammals and medaka in mTECs [28]. *ccl25b*, highly expressed in mTECs, is requested for recruiting positively-selected thymocytes. Such a migration is mediated by CCR7 and is described as essential for establishing central tolerance. In medaka, *ccr7* is not expressed in thymus at larval stage [28]: we were also unable to mine this transcript by homology searches in our dataset and only found *ccr9* and *cxcr4* but, given the redundant roles revealed for Ccr9, Ccr7 and Cxcr4 in the regulation of thymus homing [114], it is possible that such a cooperation may also apply to this cortex-to-medulla scenario. To increase sensitivity to attractant gradients for completion of developmental steps across cortex and medulla and for peripheral navigation, T cells can up-regulate the cell surface expression of GPCRs (G-protein–coupled receptors) which, upon agonist binding, induce intracellular pro-migratory responses [115]. According to our GSEA results, the "GPCR downstream signaling" gene set was significantly enriched in the medulla and was associated with the highest number of core genes (i.e. 19 %) influencing the enrichment score (Fig. 4B and 5B).

Aire up-regulated gene expression in the sea bass medulla contributed to the over-representation of several immune-related biological processes such as "regulation of immune system process", "T cell activation" and "leukocyte differentiation" (Table S4B). The pivotal roles of mammalian Aire have been elucidated in detail in recent years. Aire i) is a master inducer of self-antigens such as tissue-restricted/specific antigens (TRAs/TSAs) for T cell negative selection purposes by facilitating the interaction between many transcriptional regulators and histone H3 [78], ii) promotes alternative mRNA splicing of TSAs that leads to diversification of the thymus immunopeptidome [116], iii) regulates interactions between maturing lymphocytes and TECs by promoting thymic crosstalk [117] and iv) controls TEC maturation [118] or the expression of Ccr7 and Ccr4 ligands (i.e. Ccl25b and Cxcl12) [119]. It must be also mentioned, though, that TRAs may be also directly induced by Fez family zinc finger 2 (*fezf2*) transcriptional regulator [78], for which we could not gather any data likely due to its poor 3' UTR annotation in the genome despite deposited in GenBank (XP_051270977.1).

Under the control of RANK and CD40, two TNF receptor family members [120], mammalian Aire is selectively expressed with the greatest extent in the thymus, in approximately 30 % of mTECs but never in cTECs. Worthy of note, *aire* is also strongly expressed in the subset of human $CD27^{-}IgM^{+}$ B cells that differentiate in the thymus and act as potent APCs to autoreactive T cells [121,122], and in aDCs, a new subtype of human DCs [84]. On this, Aire evolution was tightly linked to the arising of T and B cell-dependent adaptive immunity [123].

The heterogeneity of medullary epithelial cells subpopulations was recently elucidated by single-cell transcriptomics: *aire* is expressed at high levels and briefly only at stage-II mTECs together with thousands of self-antigens, MHC-II and co-stimulatory molecules such as CD80/CD86, which are all critical for central tolerance induction. Notably, one of the most DE genes resulted from the medulla transcriptome encoded for nattectin (Fig. 2B, Table 2), which is able to up-regulate the expression of MHC class II, CD80, CD86 and CD40 molecules [124]. During this time, cells are inclined towards apoptosis and differentiation: contrary to what initially thought, indeed, mTECs differentiation extends beyond this stage to reach the mTEC III $Aire^{+}$ lineage, which sees a down-regulation of all above-mentioned stage-II markers and a

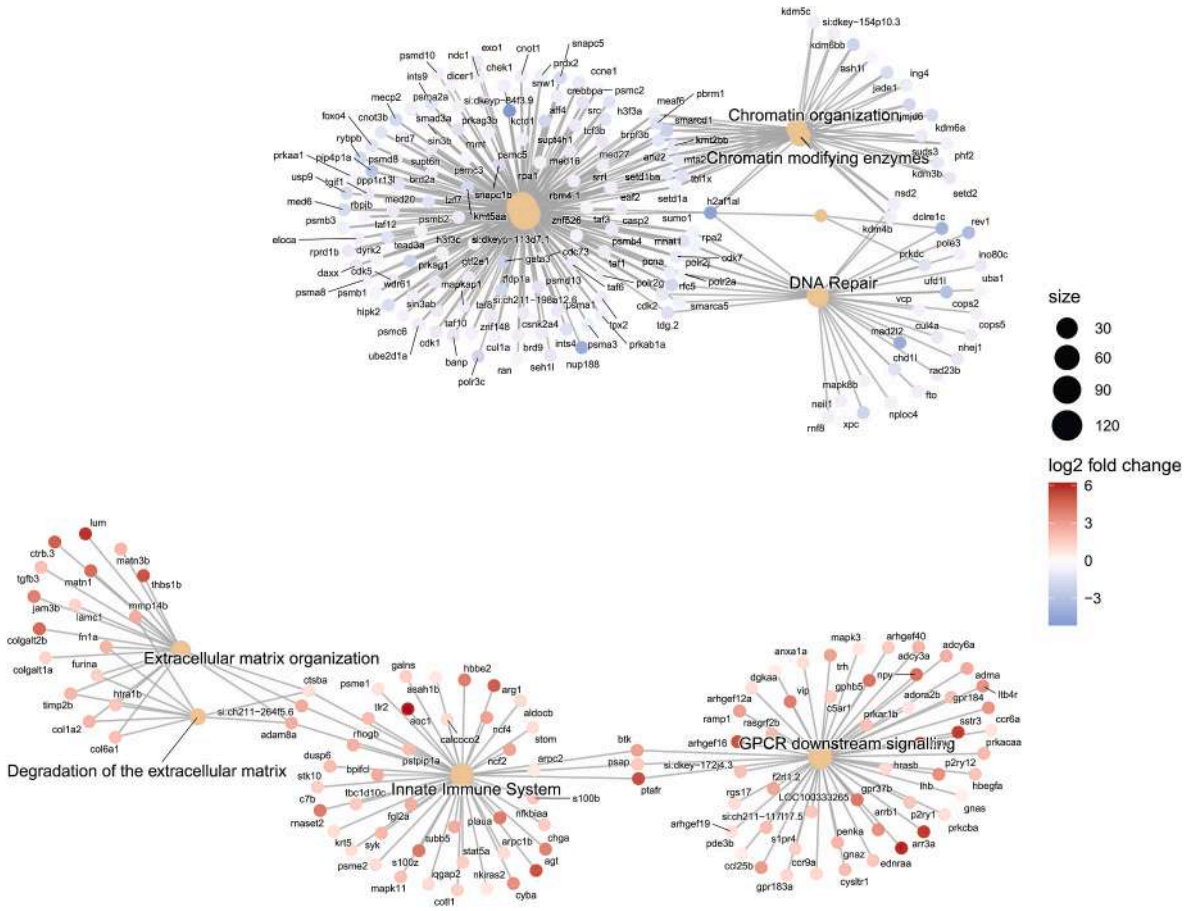

Fig. 5. (*continued*).

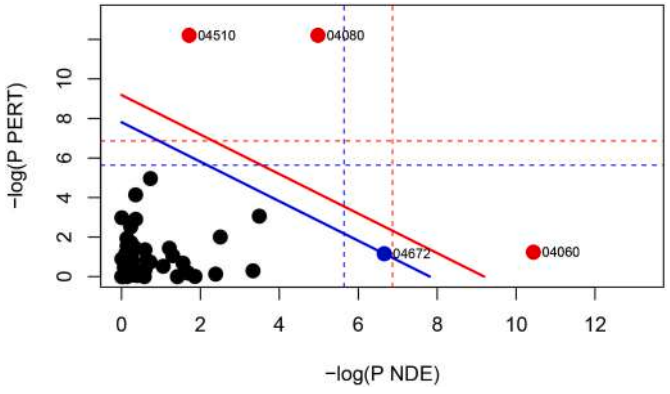

Fig. 6. Two-way evidence plot illustrating the relationship between pathway perturbation (P PERT) and over-representation (P NDE) considered by the SPIA algorithm. Each KEGG pathway tested is represented by a dot: 04510: "Focal adhesion"; 04080: "Neuroactive ligand-receptor interaction"; 04060: "Cytokine-cytokine receptor interaction"; 4672: "Intestinal immune network for IgA production". Pathways above the oblique red and blue lines are significant at 5 % after Bonferroni and FDR correction, respectively. Vertical and horizontal red and blue thresholds represent the same corrections for the two types of evidence considered individually.

concomitant transition towards a corneocyte-like phenotype achieved with the selective expression of a variety of keratins [125,126]. This is consistent with the observation of cornified bodies within the human thymus, known as Hassall's corpuscles (HCs). Several genes encoding for keratins were retrieved and homology-identified (Table 3, Tables S1A-B, S3) in our dataset: all but one (i.e. *krt94*) were over-expressed in the medulla compared to the cortex, with $\log_2$ FC ranging between 0.003 and 4.86, and 5 of them were differentially expressed. HCs were identified in some teleosts such as Channel catfish [127], *Diplodus puntazzo* [128] and Tilapia [129]. In one-year old sea bass medulla, Hassall's corpuscle-like structures were observed by immunoreactivity against CK and S100 [29]. The last post-Aire mTEC differentiation stage is mTEC IV, also known as thymic tuft cells, that produce IL-25 [130]. Thymic tuft cells have an expression profile that is strikingly similar to those of intestinal tuft cells, and were demonstrated to be involved and play vital roles in immune responses such as antigen presentation, immune tolerance, and type 2 immunity [131]. The positive perturbation of the KEGG pathway "Intestinal immune network for IgA production" (Fig. 6) may be ascribable to a tuft-like mTEC population, even though accepted biomarkers of such a population (e.g. *plcg2/plcb2* and *trpm5* of the canonical taste transduction pathway or *dclk1*), despite being more expressed in the medulla, were not DE (Table S1B). Functional information on the two above highly specialized epithelial subsets remain rather scarce.

T cells that do not pass checkpoints in the cortex (β and positive selections) and in the medulla (negative selection) are removed by apoptosis. Positive regulation of the apoptotic process resulted in the global over-representation analysis (Table S4A). Macrophages are crucial for clearing apoptotic thymocytes and maintaining thymic homeostasis. Both *mpeg1*, a recognized marker of phagocytic macrophages [132], and the gene sets of "Innate immune system" and "Toll-like receptor signaling pathway" (part of the germ-line encoded pattern recognition receptors (PRR), through which innate cells become activated) were over-expressed and enriched in the sea bass medulla (Table S1A, Fig. 4A–B, Fig. S2G). In the medulla, apoptosis is intrinsically tied to the generation of regulatory T-cells (Treg, enforcer of

self-tolerance) through a TGFβ–Foxp3 axis [133]. Sensing and uptake of apoptotic cells result in intra-thymic production of TGFβ, a cytokine that initiates and maintains Foxp3 expression in $CD4^+$ SP thymocytes [134]. Causal relationships were indeed observed: enhanced and decreased levels of apoptosis in the thymus resulted in augmented and reduced Treg populations, respectively, and TGFβ inhibition led to decreased *foxp3* mRNA, altogether rejecting this as a mere TCR-instructive process. Worthy of note, teleost thymic B cells are able to present self-antigens to $CD4^+$ thymocytes through MHC-II and engagement of CD40/CD40L [135,136] possibly to induce, as in mammalian counterparts, either clonal deletion of self-reactive thymocytes or Treg generation [137]. Understanding of regulatory T-cells in teleost is still one of the open questions in the field of T-cell development [28]: our work suggests Treg presence and the above active self-tolerance-related mechanisms in the sea bass, because i) over-representation of apoptosis (Table S4B), ii) differential expression of *tgfb*, related receptors, *foxp3*, *cd40*, *cd40l* and *cd79* (Table 3, Table S1A) and iii) activation the cytokine-cytokine receptor interaction KEGG pathway, encompassing *tgfb* (Fig. 6 and Table S8 - browse related KEGGLINK), were all seen in the medulla.

The relationship between the extracellular matrix (ECM) and thymopoiesis has started to unravel recently, and it is becoming clear that the former does not just provide physical support [138]. Thymocytes interact with TECs and fibroblasts, which actively produce ECM molecules such as several types of collagens, laminins, fibronectin and lumican, and use integrins to adhere to and receive signals from ECM components. Fibroblasts contribute to providing self-antigen for central immune tolerance [139]. Laminin can additionally bind to some cytokines, possibly representing an additional mechanism by which this extracellular matrix component modulates the behavior of T lymphocytes [140], especially considering the varying ability of thymocytes to produce cytokines and express cytokine receptors depending on their maturation stage [87]. Extracellular matrix fragments also act as chemoattractants that contribute to regulating leukocyte motility, migration, chemotaxis, positioning and cell-cell interaction [115]. In our dataset, the most DE genes in the medulla encoded for C1q domain-containing proteins that are expressed in collagen-producing cells (Fig. 2A, Table 2). We also saw an enrichment in gene sets related to organization and degradation of the extracellular matrix (Fig. 4B), with *fibronectin 1a*, *laminin subunit gamma 1*, *collagen type I isoforms* and *lumican* (i.e. common fibroblast markers [141]) identified as core enrichment genes (Fig. 5B), as well as the activation of the focal adhesion and the cytokine-cytokine receptor interaction pathways (Fig. 6, Table S8 - browse related KEGGLINK) in the medulla.

The T cell developmental journey culminates with T cell emigration, an essential step for ensuring immunological homeostasis. While little information on the mechanisms and molecules involved in the egress of thymocytes from fish thymus is available [28], throughout their time within the medulla and especially at final intra-thymic maturation, SP thymocytes acquire egress-competence by modulating the expression of specific genes. The chemokine receptor Cxcr4 and its ligand Cxcl12 are important molecules involved in thymus egress [142]. Our data showed the medullary differential expression of *cxcr4* but not of *cxcl12* (Table 3, Table S1b), suggesting that also in sea bass, like in mammals, such chemokine pair is involved both in progenitor homing [10] and T cell egress. A greater, statistically-supported expression in the medulla of sphingosine-1-phosphate receptor 4 (*s1pr4*) was also found: receptors S1PRs are responsible for the peripheral egress of mature thymocytes [143] that are attracted by a gradient of the lipid molecule produced by sphingosine-1-phosphate $(S1P)^+$ stromal cells.

5. Conclusions

The transcriptome profiling revealed significant differences in gene expression patterns between the cortical and medullary regions, indicating distinct functional roles and canonical markers of cell populations. The differential gene expression patterns observed in our study align with the idea that the cortex is engaged in processes related to early T cell development, chromatin remodeling, cell cycle regulation and antigen processing. One of the notable findings is the overexpression and enrichment of genes and pathways related to lymphocyte development and TCR signaling in the cortical region. This enrichment reflects the extensive proliferation and differentiation of thymocytes occurring in the cortex. The high expression of genes encoding transmembrane (co)receptors, with related signaling pathways, further supports the active selection and maturation of T cells within the cortical microenvironment. The medulla instead appeared as a site of antigen presentation for strict immune education. The enrichment of pathways involved in autoimmune regulation, immunological tolerance and extracellular matrix organization confirms the role of the medulla in central tolerance mechanisms, including negative selection and deletion of autoreactive T cells, also in the European sea bass, and supports the involvement of the medulla in shaping the T cell repertoire.

The in-depth data mining revealed several novel genes, including specific transcription factors and cytokines, that displayed region-specific expression signatures within the thymus. These genes may play crucial roles in coordinating the cellular interactions and molecular processes, and underscore the unique microenvironments that are critical for the proper maturation and selection of T cells. Information and annotations generated within the present study will certainly serve in future functional studies of these genes to help elucidate their precise contributions to thymic development and T cell maturation in *Dicentrarchus labrax*.

By considering established teleost experimental models (i.e. zebrafish and medaka) as well as mouse and humans, it is also possible to draw parallels between our findings and the broader understanding of thymic function in vertebrates. This agrees with the high degree of specialization in immune activities derived as incremental layers along evolution [144,145].

At last, the spatial mapping of the cortical and medullary signatures provides the first comprehensive transcriptome profiles of the European sea bass thymus, and correlates the distinctive anatomical organization of the two regions to their functional specialization. We believe these findings are valuable as they contribute to our understanding of the molecular mechanisms of the immune system and T cell maturation in teleosts, and provide a foundation for further investigations into thymic development, T cell biology and adaptive immune response regulation.

Ethics

Animal manipulation complied with the guidelines of the European Union Directive (2010/63/EU) and the Italian Legislative Decree 26 of March 4, 2014 “Attuazione della Direttiva 2010/63/UE sulla protezione degli animali utilizzati a fini scientifici”. Ethical review and approval were not required because fish were sampled from an aquaculture facility and were not subject to any experimental manipulation, in line with the Explanatory Note of the Italian Ministry of Health’s Directorate- General for Animal Health and Veterinary Medicinal Products (DGSAF) of July 26, 2017.

CRediT authorship contribution statement

A. Miccoli: Conceptualization, Formal analysis, Visualization, Data curation, Writing – original draft, Writing – review & editing. **V. Pianese:** Investigation, Visualization. **C. Bidoli:** Investigation. **A.M. Fausto:** Writing – review & editing. **G. Scapigliati:** Writing – review & editing. **S. Picchietti:** Conceptualization, Writing – original draft, Writing – review & editing, Supervision, All authors have read and agreed to the published version of the manuscript.

Data availability

Raw sequencing data is available at the NCBI SRA database under the

BioProject accession number PRJNA1001662.

Acknowledgements

This research was partially supported by the "Department of Excellence-2018" Program (Dipartimenti di Eccellenza) of the Italian Ministry of Education, University and Research, DIBAF - Department for Innovation in Biological, Agro-food and Forest Systems, University of Tuscia, Project "Landscape 4.0 – food, wellbeing and environment".

Appendix A. Supplementary data

Supplementary data to this article can be found online at https://doi.org/10.1016/j.fsi.2023.109319.

References

[1] T. Boehm, J.B. Swann, Origin and evolution of adaptive immunity, Annu. Rev. Anim. Biosci. 2 (2014) 259–283, https://doi.org/10.1146/annurev-animal-022513-114201.
[2] M.D. Cooper, M.N. Alder, The evolution of adaptive immune systems, Cell 124 (2006) 815–822, https://doi.org/10.1016/j.cell.2006.02.001.
[3] M.F. Flajnik, M. Kasahara, Origin and evolution of the adaptive immune system: genetic events and selective pressures, Nat. Rev. Genet. 11 (2010) 47–59, https://doi.org/10.1038/nrg2703.
[4] P. Dehal, J.L. Boore, Two rounds of whole genome duplication in the ancestral vertebrate, PLoS Biol. 3 (2005) e314, https://doi.org/10.1371/journal.pbio.0030314.
[5] L.Z. Holland, D. Ocampo Daza, A new look at an old question: when did the second whole genome duplication occur in vertebrate evolution? Genome Biol. 19 (2018) 209, https://doi.org/10.1186/s13059-018-1592-0.
[6] Y. Zhang, T.C. Cheng, G. Huang, Q. Lu, M.D. Surleac, J.D. Mandell, P. Pontarotti, A.J. Petrescu, A. Xu, Y. Xiong, D.G. Schatz, Transposon molecular domestication and the evolution of the RAG recombinase, Nature 569 (2019) 79–84, https://doi.org/10.1038/s41586-019-1093-7.
[7] Y. Sutoh, M. Kasahara, The immune system of jawless vertebrates: insights into the prototype of the adaptive immune system, Immunogenetics 73 (2021) 5–16, https://doi.org/10.1007/s00251-020-01182-6.
[8] G. Scapigliati, A. Miccoli, F. Buonocore, A.M. Fausto, S. Picchietti, Lymphocytes of teleosts, in: K. Buchmann, C.J. Secombes (Eds.), Princ. Fish Immunol., Springer International Publishing, 2022, pp. 177–201, https://doi.org/10.1007/978-3-030-85420-1_5.
[9] M.F. Flajnik, A cold-blooded view of adaptive immunity, Nat. Rev. Immunol. 18 (2018) 438–453, https://doi.org/10.1038/s41577-018-0003-9.
[10] T. Boehm, I. Hess, J.B. Swann, Evolution of lymphoid tissues, Trends Immunol. 33 (2012) 315–321, https://doi.org/10.1016/j.it.2012.02.005.
[11] N. Olsen Saraiva Camara, A.P. Lepique, A.S. Basso, Lymphocyte differentiation and effector functions, Clin. Dev. Immunol. 2012 (2012) 1–3, https://doi.org/10.1155/2012/510603.
[12] D. Parra, F. Takizawa, J.O. Sunyer, Evolution of B cell immunity, Annu. Rev. Anim. Biosci. 1 (2013) 65–97, https://doi.org/10.1146/annurev-animal-031412-103651.
[13] C.D. Mitchell, M.F. Criscitiello, Comparative study of cartilaginous fish divulges insights into the early evolution of primary, secondary and mucosal lymphoid tissue architecture, Fish Shellfish Immunol. 107 (2020) 435–443, https://doi.org/10.1016/j.fsi.2020.11.006.
[14] S. Chilmonczyk, The thymus in fish: development and possible function in the immune response, Annu. Rev. Fish Dis. 2 (1992) 181–200, https://doi.org/10.1016/0959-8030(92)90063-4.
[15] B. Bajoghli, P. Guo, N. Aghaallaei, M. Hirano, C. Strohmeier, N. McCurley, D. E. Bockman, M. Schorpp, M.D. Cooper, T. Boehm, A thymus candidate in lampreys, Nature 470 (2011) 90–94, https://doi.org/10.1038/nature09655.
[16] T. Boehm, C.C. Bleul, The evolutionary history of lymphoid organs, Nat. Immunol. 8 (2007) 131–135, https://doi.org/10.1038/ni1435.
[17] F. Barraza, R. Montero, V. Wong-Benito, H. Valenzuela, C. Godoy-Guzmán, F. Guzmán, B. Köllner, T. Wang, C.J. Secombes, K. Maisey, M. Imarai, Revisiting the teleost thymus: current knowledge and future perspectives, Biology 10 (2020) 8, https://doi.org/10.3390/biology10010008.
[18] P. Thapa, D.L. Farber, The role of the thymus in the immune response, Thorac. Surg. Clin. 29 (2019) 123–131, https://doi.org/10.1016/j.thorsurg.2018.12.001.
[19] D. Ma, Y. Wei, F. Liu, Regulatory mechanisms of thymus and T cell development, Dev. Comp. Immunol. 39 (2013) 91–102, https://doi.org/10.1016/j.dci.2011.12.013.
[20] R. Morimoto, J. Swann, A. Nusser, I. Trancoso, M. Schorpp, T. Boehm, Evolution of thymopoietic microenvironments, Open Biol 11 (2021), https://doi.org/10.1098/rsob.200383.
[21] Q. Ge, Y. Zhao, Evolution of thymus organogenesis, Dev. Comp. Immunol. 39 (2013) 85–90, https://doi.org/10.1016/j.dci.2012.01.002.
[22] M. Itoi, N. Tsukamoto, H. Yoshida, T. Amagai, Mesenchymal cells are required for functional development of thymic epithelial cells, Int. Immunol. 19 (2007) 953–964, https://doi.org/10.1093/intimm/dxm060.
[23] A. Zapata, C.T. Amemiya, Phylogeny of lower vertebrates and their immunological structures, Curr. Top. Microbiol. Immunol. (2000) 67–107, https://doi.org/10.1007/978-3-642-59674-2_5.
[24] J. Gordon, N.R. Manley, Mechanisms of thymus organogenesis and morphogenesis, Development 138 (2011) 3865–3878, https://doi.org/10.1242/dev.059998.
[25] T.J. Bowden, P. Cook, J.H.W.M. Rombout, Development and function of the thymus in teleosts, Fish Shellfish Immunol. 19 (2005) 413–427, https://doi.org/10.1016/j.fsi.2005.02.003.
[26] H. Bjørgen, E.O. Koppang, Anatomy of teleost fish immune structures and organs, Immunogenetics 73 (2021) 53–63, https://doi.org/10.1007/s00251-020-01196-0.
[27] A.G. Zapata, A. Chibá, A. Varas, Cells and tissues of the immune system of fish, in: G. Iwama, T. Nakanishi (Eds.), Fish Physiol., Elsevier B.V, 1996, pp. 1–62, https://doi.org/10.1016/S1546-5098(08)60271-X.
[28] B. Bajoghli, A.M. Dick, A. Claasen, L. Doll, N. Aghaallaei, Zebrafish and medaka: two teleost models of T-cell and thymic development, Int. J. Mol. Sci. 20 (2019), https://doi.org/10.3390/ijms20174179.
[29] M. Paiola, T. Knigge, S. Picchietti, A. Duflot, L. Guerra, P.I.S. Pinto, G. Scapigliati, T. Monsinjon, Oestrogen receptor distribution related to functional thymus anatomy of the European sea bass, Dicentrarchus labrax, Dev. Comp. Immunol. 77 (2017) 106–120, https://doi.org/10.1016/j.dci.2017.07.023.
[30] L. Abelli, S. Picchietti, N. Romano, L. Mastrolia, G. Scapigliati, Immunocytochemical detection of thymocyte antigenic determinants in developing lymphoid organs of sea bass dicentrarchus labrax (L.), Fish Shellfish Immunol. 6 (1996) 493–505, https://doi.org/10.1006/fsim.1996.0047.
[31] L. Abelli, S. Picchietti, N. Romano, L. Mastrolia, G. Scapigliati, Ontogeny of thymocytes in sea bass dicentrarchus labrax: studies with monoclonal antibodies, Ital. J. Zool. 63 (1996) 329–331, https://doi.org/10.1080/11250009609356154.
[32] F. Buonocore, R. Castro, E. Randelli, M.-P. Lefranc, A. Six, H. Kuhl, R. Reinhardt, A. Facchiano, P. Boudinot, G. Scapigliati, Diversity, molecular characterization and expression of T cell receptor γ in a teleost fish, the sea bass (Dicentrarchus labrax, L), PLoS One 7 (2012), e47957, https://doi.org/10.1371/journal.pone.0047957.
[33] F. Buonocore, E. Randelli, D. Casani, L. Guerra, S. Picchietti, S. Costantini, A. M. Facchiano, J. Zou, C.J. Secombes, G. Scapigliati, A CD4 homologue in sea bass (Dicentrarchus labrax): molecular characterization and structural analysis, Mol. Immunol. 45 (2008) 3168–3177, https://doi.org/10.1016/j.molimm.2008.02.024.
[34] E. Randelli, G. Scapigliati, F. Buonocore, CD3γ/δ in sea bass (Dicentrarchus labrax): molecular characterization and expression analysis, Results Immunol 1 (2011) 31–35, https://doi.org/10.1016/j.rinim.2011.08.003.
[35] F. Buonocore, E. Randelli, S. Bird, C.J. Secombes, S. Costantini, A. Facchiano, M. Mazzini, G. Scapigliati, The CD8α from sea bass (Dicentrarchus labrax L.): cloning, expression and 3D modelling, Fish Shellfish Immunol. 20 (2006) 637–646, https://doi.org/10.1016/j.fsi.2005.08.006.
[36] F. Buonocore, E. Randelli, D. Casani, S. Costantini, A. Facchiano, G. Scapigliati, R. Stet, Molecular cloning, differential expression and 3D structural analysis of the MHC class-II β chain from sea bass (Dicentrarchus labrax L.), Fish Shellfish Immunol. 23 (2007) 853–866, https://doi.org/10.1016/j.fsi.2007.03.013.
[37] S. Picchietti, L. Abelli, L. Guerra, E. Randelli, F. Proietti Serafini, M. C. Belardinelli, F. Buonocore, C. Bernini, A.M. Fausto, G. Scapigliati, MHC II-β chain gene expression studies define the regional organization of the thymus in the developing bony fish Dicentrarchus labrax (L.), Fish Shellfish Immunol. 42 (2015) 483–493, https://doi.org/10.1016/j.fsi.2014.11.012.
[38] S. Picchietti, L. Guerra, F. Buonocore, E. Randelli, A.M. Fausto, L. Abelli, Lymphocyte differentiation in sea bass thymus: CD4 and CD8-α gene expression studies, Fish Shellfish Immunol. 27 (2009) 50–56, https://doi.org/10.1016/j.fsi.2009.04.003.
[39] S. Picchietti, L. Guerra, L. Selleri, F. Buonocore, L. Abelli, G. Scapigliati, M. Mazzini, A.M. Fausto, Compartmentalisation of T cells expressing CD8α and TCRβ in developing thymus of sea bass Dicentrarchus labrax (L.), Dev. Comp. Immunol. 32 (2008) 92–99, https://doi.org/10.1016/j.dci.2007.04.002.
[40] S. Picchietti, F. Buonocore, L. Guerra, M.C. Belardinelli, T. De Wolf, A. Couto, A. M. Fausto, P.R. Saraceni, A. Miccoli, G. Scapigliati, Molecular and cellular characterization of European sea bass CD3ε+ T lymphocytes and their modulation by microalgal feed supplementation, Cell Tissue Res. 384 (2021) 149–165, https://doi.org/10.1007/s00441-020-03347-x.
[41] A. Miccoli, L. Guerra, V. Pianese, P.R. Saraceni, F. Buonocore, A.R. Taddei, A. Couto, T. De Wolf, A.M. Fausto, G. Scapigliati, S. Picchietti, Molecular, cellular and functional analysis of TRγ chain along the European sea bass Dicentrarchus labrax development, Int. J. Mol. Sci. 22 (2021) 3376, https://doi.org/10.3390/ijms22073376.
[42] A. Miccoli, F. Buonocore, S. Picchietti, G. Scapigliati, The sea bass Dicentrarchus labrax as a marine model species in immunology : insights from basic and applied research, Aquac. Fish. (2021), https://doi.org/10.1016/j.aaf.2021.09.003.
[43] V. Espina, J.D. Wulfkuhle, V.S. Calvert, A. VanMeter, W. Zhou, G. Coukos, D. H. Geho, E.F. Petricoin, L.A. Liotta, Laser-capture microdissection, Nat. Protoc. 1 (2006) 586–603, https://doi.org/10.1038/nprot.2006.85.
[44] S. Picchietti, L. Guerra, F. Bertoni, E. Randelli, M.C. Belardinelli, F. Buonocore, A. M. Fausto, J.H. Rombout, G. Scapigliati, L. Abelli, Intestinal T cells of Dicentrarchus labrax (L.): gene expression and functional studies, Fish Shellfish Immunol. 30 (2011) 609–617, https://doi.org/10.1016/j.fsi.2010.12.006.
[45] F. Buonocore, E. Randelli, P. Tranfa, G. Scapigliati, A CD83-like molecule in sea bass (Dicentrarchus labrax): molecular characterization and modulation by viral

and bacterial infection, Fish Shellfish Immunol. 32 (2012) 1179–1184, https://doi.org/10.1016/j.fsi.2012.02.027.
[46] M.I. Love, W. Huber, S. Anders, Moderated estimation of fold change and dispersion for RNA-seq data with DESeq2, Genome Biol. 15 (2014) 550, https://doi.org/10.1186/s13059-014-0550-8.
[47] Ying Sha, J.H. Phan, M.D. Wang, Effect of low-expression gene filtering on detection of differentially expressed genes in RNA-seq data, in: 2015 37th Annu. Int. Conf. IEEE Eng. Med. Biol. Soc., IEEE, 2015, pp. 6461–6464, https://doi.org/10.1109/EMBC.2015.7319872.
[48] A. Zhu, J.G. Ibrahim, M.I. Love, Heavy-tailed prior distributions for sequence count data: removing the noise and preserving large differences, Bioinformatics 35 (2019) 2084–2092, https://doi.org/10.1093/bioinformatics/bty895.
[49] S. Durinck, P.T. Spellman, E. Birney, W. Huber, Mapping identifiers for the integration of genomic datasets with the R/Bioconductor package biomaRt, Nat. Protoc. 4 (2009) 1184–1191, https://doi.org/10.1038/nprot.2009.97.
[50] T. Wu, E. Hu, S. Xu, M. Chen, P. Guo, Z. Dai, T. Feng, L. Zhou, W. Tang, L. Zhan, X. Fu, S. Liu, X. Bo, G. Yu, clusterProfiler 4.0: a universal enrichment tool for interpreting omics data, Innov 2 (2021), 100141, https://doi.org/10.1016/j.xinn.2021.100141.
[51] G. Yu, Q.-Y. He, ReactomePA: an R/Bioconductor package for reactome pathway analysis and visualization, Mol. Biosyst. 12 (2016) 477–479, https://doi.org/10.1039/C5MB00663E.
[52] G. Yu, Visualization of functional enrichment result, R package 3 (2023) enrichplot:, version 1.20.
[53] W. Luo, C. Brouwer, Pathview: an R/Bioconductor package for pathway-based data integration and visualization, Bioinformatics 29 (2013) 1830–1831, https://doi.org/10.1093/bioinformatics/btt285.
[54] A. Subramanian, P. Tamayo, V.K. Mootha, S. Mukherjee, B.L. Ebert, M.A. Gillette, A. Paulovich, S.L. Pomeroy, T.R. Golub, E.S. Lander, J.P. Mesirov, Gene set enrichment analysis: a knowledge-based approach for interpreting genome-wide expression profiles, Proc. Natl. Acad. Sci. USA 102 (2005) 15545–15550, https://doi.org/10.1073/pnas.0506580102.
[55] M. Carlson, org.Dr.eg.db: Genome Wide Annotation for Zebrafish. R Package, 2023, version 3.17.0.
[56] J. Reimand, R. Isserlin, V. Voisin, M. Kucera, C. Tannus-Lopes, A. Rostamianfar, L. Wadi, M. Meyer, J. Wong, C. Xu, D. Merico, G.D. Bader, Pathway enrichment analysis and visualization of omics data using g:Profiler, GSEA, Cytoscape and EnrichmentMap, Nat. Protoc. 14 (2019) 482–517, https://doi.org/10.1038/s41596-018-0103-9.
[57] A.L. Tarca, S. Draghici, P. Khatri, S.S. Hassan, P. Mittal, J.S. Kim, C.J. Kim, J. P. Kusanovic, R. Romero, A novel signaling pathway impact analysis, Bioinformatics 25 (2009) 75–82, https://doi.org/10.1093/bioinformatics/btn577.
[58] A.L. Tarca, P. Kathri, S. Draghici, SPIA: signaling Pathway Impact Analysis (SPIA) using combined evidence of pathway over-representation and unusual signaling perturbations, R package (2023), version 2.52.0.
[59] C. Camacho, G. Coulouris, V. Avagyan, N. Ma, J. Papadopoulos, K. Bealer, T. L. Madden, BLAST+: architecture and applications, BMC Bioinf. 10 (2009) 421, https://doi.org/10.1186/1471-2105-10-421.
[60] I. Letunic, S. Khedkar, P. Bork, SMART: recent updates, new developments and status in 2020, Nucleic Acids Res. 49 (2021) D458–D460, https://doi.org/10.1093/nar/gkaa937.
[61] T. Paysan-Lafosse, M. Blum, S. Chuguransky, T. Grego, B.L. Pinto, G.A. Salazar, M.L. Bileschi, P. Bork, A. Bridge, L. Colwell, J. Gough, D.H. Haft, I. Letunić, A. Marchler-Bauer, H. Mi, D.A. Natale, C.A. Orengo, A.P. Pandurangan, C. Rivoire, C.J.A. Sigrist, I. Sillitoe, N. Thanki, P.D. Thomas, S.C.E. Tosatto, C. H. Wu, A. Bateman, InterPro in 2022, Nucleic Acids Res. 51 (2023) D418–D427, https://doi.org/10.1093/nar/gkac993.
[62] A. Cambi, C.G. Figdor, Dual function of C-type lectin-like receptors in the immune system, Curr. Opin. Cell Biol. 15 (2003) 539–546, https://doi.org/10.1016/j.ceb.2003.08.004.
[63] L.J. Zhou, T.F. Tedder, Human blood dendritic cells selectively express CD83, a member of the immunoglobulin superfamily, J. Immunol. 154 (1995) 3821–3835, https://doi.org/10.4049/jimmunol.154.8.3821.
[64] Y. Kuwano, C.M. Prazma, N. Yazawa, R. Watanabe, N. Ishiura, A. Kumanogoh, H. Okochi, K. Tamaki, M. Fujimoto, T.F. Tedder, CD83 influences cell-surface MHC class II expression on B cells and other antigen-presenting cells, Int. Immunol. 19 (2007) 977–992, https://doi.org/10.1093/intimm/dxm067.
[65] A.N. Rogers, D.G. VanBuren, E.E. Hedblom, M.E. Tilahun, J.C. Telfer, C. L. Baldwin, Γδ T cell function varies with the expressed WC1 coreceptor, J. Immunol. 174 (2005) 3386–3393, https://doi.org/10.4049/jimmunol.174.6.3386.
[66] D.R. Flower, Multiple molecular recognition properties of the lipocalin protein family, J. Mol. Recogn. 8 (1995) 185–195, https://doi.org/10.1002/jmr.300080304.
[67] D.R. Flower, The lipocalin protein family: structure and function, Biochem. J. 318 (1996) 1–14, https://doi.org/10.1042/bj3180001.
[68] D. Schubert, M. LaCorbiere, Isolation of an adhesion-mediating protein from chick neural retina adherons, J. Cell Biol. 101 (1985) 1071–1077, https://doi.org/10.1083/jcb.101.3.1071.
[69] P. Berman, P. Gray, E. Chen, K. Keyser, D. Ehrlich, H. Karten, M. LaCorbiere, F. Esch, D. Schubert, Sequence analysis, cellular localization, and expression of a neuroretina adhesion and cell survival molecule, Cell 51 (1987) 135–142, https://doi.org/10.1016/0092-8674(87)90018-3.
[70] E. Anguita, F.J. Candel, A. Chaparro, J.J. Roldán-Etcheverry, Transcription factor GFI1B in Health and disease, Front. Oncol. 7 (2017), https://doi.org/10.3389/fonc.2017.00054.
[71] F. Le Deist, C. Poinsignon, D. Moshous, A. Fischer, J.-P. de Villartay, Artemis sheds new light on V(D)J recombination, Immunol. Rev. 200 (2004) 142–155, https://doi.org/10.1111/j.0105-2896.2004.00169.x.
[72] C. Poinsignon, D. Moshous, I. Callebaut, R. de Chasseval, I. Villey, J.-P. de Villartay, The metallo-β-lactamase/β-CASP domain of artemis constitutes the catalytic core for V(D)J recombination, J. Exp. Med. 199 (2004) 315–321, https://doi.org/10.1084/jem.20031142.
[73] M. Frantzeskakis, Y. Takahama, I. Ohigashi, The role of proteasomes in the thymus, Front. Immunol. 12 (2021) 1–6, https://doi.org/10.3389/fimmu.2021.646209.
[74] A. Apavaloaei, S. Brochu, M. Dong, A. Rouette, M.-P. Hardy, G. Villafano, S. Murata, H.J. Melichar, C. Perreault, PSMB11 orchestrates the development of CD4 and CD8 thymocytes via regulation of gene expression in cortical thymic epithelial cells, J. Immunol. 202 (2019) 966–978, https://doi.org/10.4049/jimmunol.1801288.
[75] L. Tian, S.A. Greenberg, S.W. Kong, J. Altschuler, I.S. Kohane, P.J. Park, Discovering statistically significant pathways in expression profiling studies, Proc. Natl. Acad. Sci. USA 102 (2005) 13544–13549, https://doi.org/10.1073/pnas.0506577102.
[76] B. Bajoghli, N. Aghaallaei, I. Hess, I. Rode, N. Netuschil, B.-H. Tay, B. Venkatesh, J.-K. Yu, S.L. Kaltenbach, N.D. Holland, D. Diekhoff, C. Happe, M. Schorpp, T. Boehm, Evolution of genetic networks underlying the emergence of thymopoiesis in vertebrates, Cell 138 (2009) 186–197, https://doi.org/10.1016/j.cell.2009.04.017.
[77] M.F. Criscitiello, Y. Ohta, M. Saltis, E.C. McKinney, M.F. Flajnik, Evolutionarily conserved TCR binding sites, identification of T cells in primary lymphoid tissues, and surprising trans-rearrangements in nurse shark, J. Immunol. 184 (2010) 6950–6960, https://doi.org/10.4049/jimmunol.0902774.
[78] H. Takaba, H. Takayanagi, The mechanisms of T cell selection in the thymus, Trends Immunol. 38 (2017) 805–816, https://doi.org/10.1016/j.it.2017.07.010.
[79] G.L. Stritesky, Y. Xing, J.R. Erickson, L.A. Kalekar, X. Wang, D.L. Mueller, S. C. Jameson, K.A. Hogquist, Murine thymic selection quantified using a unique method to capture deleted T cells, Proc. Natl. Acad. Sci. U.S.A. 110 (2013) 4679–4684, https://doi.org/10.1073/pnas.1217532110.
[80] J.W. Kappler, N. Roehm, P. Marrack, T cell tolerance by clonal elimination in the thymus, Cell 49 (1987) 273–280, https://doi.org/10.1016/0092-8674(87)90568-X.
[81] S.Z. Josefowicz, L.-F. Lu, A.Y. Rudensky, Regulatory T cells: mechanisms of differentiation and function, Annu. Rev. Immunol. 30 (2012) 531–564, https://doi.org/10.1146/annurev.immunol.25.022106.141623.
[82] J. Gameiro, P. Nagib, L. Verinaud, The thymus microenvironment in regulating thymocyte differentiation, Cell Adhes. Migrat. 4 (2010) 382–390, https://doi.org/10.4161/cam.4.3.11789.
[83] L. Calderón, T. Boehm, Synergistic, context-dependent, and hierarchical functions of epithelial components in thymic microenvironments, Cell 149 (2012) 159–172, https://doi.org/10.1016/j.cell.2012.01.049.
[84] H. Wang, J.C. Zúñiga-Pflücker, Thymic microenvironment: interactions between innate immune cells and developing thymocytes, Front. Immunol. 13 (2022) 1–9, https://doi.org/10.3389/fimmu.2022.885280.
[85] C.C. Bleul, T. Boehm, Chemokines define distinct microenvironments in the developing thymus, Eur. J. Immunol. 30 (2000) 3371–3379, https://doi.org/10.1002/1521-4141(2000012)30:12<3371::AID-IMMU3371>3.0.CO;2-L.
[86] I. Dzhagalov, H. Phee, How to find your way through the thymus: a practical guide for aspiring T cells, Cell, Mol. Life Sci. 69 (2012) 663–682, https://doi.org/10.1007/s00018-011-0791-6.
[87] A. Yarilin, I. Belyakov, Cytokines in the thymus: production and biological effects, Curr. Med. Chem. 11 (2005) 447–464, https://doi.org/10.2174/0929867043455972.
[88] H.-R. Rodewald, Thymus organogenesis, Annu. Rev. Immunol. 26 (2008) 355–388, https://doi.org/10.1146/annurev.immunol.26.021607.090408.
[89] E.M. Pantelouris, J. Hair, Thymus dysgenesis in nude (nu nu) mice, Development 24 (1970) 615–623, https://doi.org/10.1242/dev.24.3.615.
[90] M. Nehls, B. Kyewski, M. Messerle, R. Waldschütz, K. Schüddekopf, A.J.H. Smith, T. Boehm, Two genetically separable steps in the differentiation of thymic epithelium, Science 272 (1996) 886–889, https://doi.org/10.1126/science.272.5263.886, 80-.
[91] H.J. Vaidya, A. Briones Leon, C.C. Blackburn, FOXN1 in thymus organogenesis and development, Eur. J. Immunol. 46 (2016) 1826–1837, https://doi.org/10.1002/eji.201545814.
[92] J. Li, L.P. Wachsmuth, S. Xiao, B.G. Condie, N.R. Manley, Foxn1 overexpression promotes thymic epithelial progenitor cell proliferation and mTEC maintenance, but does not prevent thymic involution, Dev 150 (2023), https://doi.org/10.1242/dev.200995.
[93] M.L. Scimone, I. Aifantis, I. Apostolou, H. Von Boehmer, U.H. Von Andrian, A multistep adhesion cascade for lymphoid progenitor cell homing to the thymus, Proc. Natl. Acad. Sci. U.S.A. 103 (2006) 7006–7011, https://doi.org/10.1073/pnas.0602024103.
[94] U. Koch, E. Fiorini, R. Benedito, V. Besseyrias, K. Schuster-Gossler, M. Pierres, N. R. Manley, A. Duarte, H.R. MacDonald, F. Radtke, Delta-like 4 is the essential, nonredundant ligand for Notchl during thymic T cell lineage commitment, J. Exp. Med. 205 (2008) 2515–2523, https://doi.org/10.1084/jem.20080829.
[95] T. Taghon, M.A. Yui, R. Pant, R.A. Diamond, E.V. Rothenberg, Developmental and molecular characterization of emerging β- and γδ-selected pre-T cells in the adult

mouse thymus, Immunity 24 (2006) 53–64, https://doi.org/10.1016/j.immuni.2005.11.012.
[96] M. Zhang, X. Lin, Z. Yang, X. Li, Z. Zhou, P.E. Love, J. Huang, B. Zhao, Metabolic regulation of T cell development, Front. Immunol. 13 (2022) 1–9, https://doi.org/10.3389/fimmu.2022.946119.
[97] M. Ciofani, J.C. Zúñiga-Pflücker, Determining γ δ versus α β T cell development, Nat. Rev. Immunol. 10 (2010) 657–663, https://doi.org/10.1038/nri2820.
[98] K. Yang, D.B. Blanco, X. Chen, P. Dash, G. Neale, C. Rosencrance, J. Easton, W. Chen, C. Cheng, Y. Dhungana, K.C. Anil, W. Awad, X.Z.J. Guo, P.G. Thomas, H. Chi, Metabolic signaling directs the reciprocal lineage decisions of and T cells, Sci. Immunol. 3 (2018), https://doi.org/10.1126/sciimmunol.aas9818.
[99] P.A. Robert, H. Kunze-Schumacher, V. Greiff, A. Krueger, Modeling the dynamics of t-cell development in the thymus, Entropy 23 (2021), https://doi.org/10.3390/e23040437.
[100] N. Kadouri, S. Nevo, Y. Goldfarb, J. Abramson, Thymic epithelial cell heterogeneity: TEC by TEC, Nat. Rev. Immunol. 20 (2020) 239–253, https://doi.org/10.1038/s41577-019-0238-0.
[101] J. Nedjic, M. Aichinger, L. Klein, Autophagy and T cell education in the thymus: eat yourself to know yourself, Cell Cycle 7 (2008) 3625–3628, https://doi.org/10.4161/cc.7.23.7121.
[102] C. Johnstone, E. Chaves-Pozo, Antigen presentation and autophagy in teleost adaptive immunity, Int. J. Mol. Sci. 23 (2022) 1–20, https://doi.org/10.3390/ijms23094899.
[103] E.O. Koppang, I. Hordvik, I. Bjerkås, J. Torvund, L. Aune, J. Thevarajan, C. Endresen, Production of rabbit antisera against recombinant MHC class II β chain and identification of immunoreactive cells in Atlantic salmon (Salmo salar), Fish Shellfish Immunol. 14 (2003) 115–132, https://doi.org/10.1006/fsim.2002.0424.
[104] U. Fischer, J.M. Dijkstra, B. Köllner, I. Kiryu, E.O. Koppang, I. Hordvik, Y. Sawamoto, M. Ototake, The ontogeny of MHC class I expression in rainbow trout (Oncorhynchus mykiss), Fish Shellfish Immunol. 18 (2005) 49–60, https://doi.org/10.1016/j.fsi.2004.05.006.
[105] S. Murata, K. Sasaki, T. Kishimoto, S.I. Niwa, H. Hayashi, Y. Takahama, K. Tanaka, Regulation of CD8+ T cell development by thymus-specific proteasomes, Science 316 (2007) 1349–1353, https://doi.org/10.1126/science.1141915, 80-.
[106] U. Tomaru, A. Ishizu, S. Murata, Y. Miyatake, S. Suzuki, S. Takahashi, T. Kazamaki, J. Ohara, T. Baba, S. Iwasaki, K. Fugo, N. Otsuka, K. Tanaka, M. Kasahara, Exclusive expression of proteasome subunit β5t in the human thymic cortex, Blood 113 (2009) 5186–5191, https://doi.org/10.1182/blood-2008-11-187633.
[107] Y. Nakagawa, I. Ohigashi, T. Nitta, M. Sakata, K. Tanaka, S. Murata, O. Kanagawa, Y. Takahama, Thymic nurse cells provide microenvironment for secondary T cell receptor α rearrangement in cortical thymocytes, Proc. Natl. Acad. Sci. U.S.A. 109 (2012) 20572–20577, https://doi.org/10.1073/pnas.1213069109.
[108] U. Tomaru, S. Konno, S. Miyajima, R. Kimoto, M. Onodera, S. Kiuchi, S. Murata, A. Ishizu, M. Kasahara, Restricted expression of the thymoproteasome is required for thymic selection and peripheral homeostasis of CD8 + T cells, Cell Rep. 26 (2019) 639–651.e2, https://doi.org/10.1016/j.celrep.2018.12.078.
[109] I. Ohigashi, M. Frantzeskakis, A. Jacques, S. Fujimori, A. Ushio, F. Yamashita, N. Ishimaru, D. Yin, M. Cam, M.C. Kelly, P. Awasthi, K. Takada, Y. Takahama, The thymoproteasome hardwires the TCR repertoire of CD8+ T cells in the cortex independent of negative selection, J. Exp. Med. 218 (2021), https://doi.org/10.1084/JEM.20201904.
[110] K. Takada, Y. Takahama, Positive-selection-inducing self-peptides displayed by cortical thymic epithelial cells, Adv. Immunol. (2015) 87–110, https://doi.org/10.1016/bs.ai.2014.09.003.
[111] V. Sun, M. Sharpley, K.E. Kaczor-Urbanowicz, P. Chang, A. Montel-Hagen, S. Lopez, A. Zampieri, Y. Zhu, S.C. de Barros, C. Parekh, D. Casero, U. Banerjee, G. M. Crooks, The metabolic landscape of thymic T cell development in vivo and in vitro, Front. Immunol. 12 (2021), https://doi.org/10.3389/fimmu.2021.716661.
[112] M. Heino, P. Peterson, J. Kudoh, K. Nagamine, A. Lagerstedt, V. Ovod, A. Ranki, I. Rantala, M. Nieminen, J. Tuukkanen, H.S. Scott, S.E. Antonarakis, N. Shimizu, K. Krohn, Autoimmune regulator is expressed in the cells regulating immune tolerance in thymus medulla, Biochem. Biophys. Res. Commun. 257 (1999) 821–825, https://doi.org/10.1006/bbrc.1999.0308.
[113] R. Förster, A.C. Davalos-Misslitz, A. Rot, CCR7 and its ligands: balancing immunity and tolerance, Nat. Rev. Immunol. 8 (2008) 362–371, https://doi.org/10.1038/nri2297.
[114] L. Calderón, T. Boehm, Three chemokine receptors cooperatively regulate homing of hematopoietic progenitors to the embryonic mouse thymus, Proc. Natl. Acad. Sci. U.S.A. 108 (2011) 7517–7522, https://doi.org/10.1073/pnas.1016428108.
[115] T. Lämmermann, W. Kastenmüller, Concepts of GPCR-controlled navigation in the immune system, Immunol. Rev. 289 (2019) 205–231, https://doi.org/10.1111/imr.12752.
[116] G.A. Passos, C.A. Speck-Hernandez, A.F. Assis, D.A. Mendes-da-Cruz, Update on Aire and thymic negative selection, Immunology 153 (2018) 10–20, https://doi.org/10.1111/imm.12831.
[117] R. Perniola, Twenty years of AIRE, Front. Immunol. 9 (2018), https://doi.org/10.3389/fimmu.2018.00098.
[118] Y. Nishikawa, H. Nishijima, M. Matsumoto, J. Morimoto, F. Hirota, S. Takahashi, H. Luche, H.J. Fehling, Y. Mouri, M. Matsumoto, Temporal lineage tracing of aire-expressing cells reveals a requirement for aire in their maturation program, J. Immunol. 192 (2014) 2585–2592, https://doi.org/10.4049/jimmunol.1302786.
[119] M. Laan, K. Kisand, V. Kont, K. Möll, L. Tserel, H.S. Scott, P. Peterson, Autoimmune regulator deficiency results in decreased expression of CCR4 and CCR7 ligands and in delayed migration of CD4+ thymocytes, J. Immunol. 183 (2009) 7682–7691, https://doi.org/10.4049/jimmunol.0804133.
[120] T. Akiyama, M. Shinzawa, N. Akiyama, TNF receptor family signaling in the development and functions of medullary thymic epithelial cells, Front. Immunol. 3 (2012), https://doi.org/10.3389/fimmu.2012.00278.
[121] V. Gies, A. Guffroy, F. Danion, P. Billaud, C. Keime, J.D. Fauny, S. Susini, A. Soley, T. Martin, J.L. Pasquali, F. Gros, I. André-Schmutz, P. Soulas-Sprauel, A. S. Korganow, B cells differentiate in human thymus and express AIRE, J. Allergy Clin. Immunol. 139 (2017) 1049, https://doi.org/10.1016/j.jaci.2016.09.044, 1052.e12.
[122] T. Yamano, J. Nedjic, M. Hinterberger, M. Steinert, S. Koser, S. Pinto, N. Gerdes, E. Lutgens, N. Ishimaru, M. Busslinger, B. Brors, B. Kyewski, L. Klein, Thymic B cells are licensed to present self antigens for central T cell tolerance induction, Immunity 42 (2015) 1048–1061, https://doi.org/10.1016/j.immuni.2015.05.013.
[123] B. Kyewski, L. Klein, A central role for central tolerance, Annu. Rev. Immunol. 24 (2006) 571–606, https://doi.org/10.1146/annurev.immunol.23.021704.115601.
[124] E.K. Ishizuka, M.J. Ferreira, L.Z. Grund, E.M.M. Coutinho, E.N. Komegae, A. A. Cassado, K.R. Bortoluci, M. Lopes-Ferreira, C. Lima, Role of interplay between IL-4 and IFN-γ in the in regulating M1 macrophage polarization induced by Nattectin, Int. Immunopharm. 14 (2012) 513–522, https://doi.org/10.1016/j.intimp.2012.08.009.
[125] X. Wang, M. Laan, R. Bichele, K. Kisand, H.S. Scott, P. Peterson, Post-Aire maturation of thymic medullary epithelial cells involves selective expression of keratinocyte-specific autoantigens, Front. Immunol. 3 (2012), https://doi.org/10.3389/fimmu.2012.00019.
[126] S.N. Sansom, N. Shikama-Dorn, S. Zhanybekova, G. Nusspaumer, I.C. Macaulay, M.E. Deadman, A. Heger, C.P. Ponting, G.A. Holländer, Population and single-cell genomics reveal the Aire dependency, relief from Polycomb silencing, and distribution of self-antigen expression in thymic epithelia, Genome Res. 24 (2014) 1918–1931, https://doi.org/10.1101/gr.171645.113.
[127] C.F. Ellsaesser, J.E. Bly, L.W. Clem, Phylogeny of lymphocyte heterogeneity: the thymus of the channel catfish, Dev. Comp. Immunol. 12 (1988) 787–799, https://doi.org/10.1016/0145-305X(88)90053-5.
[128] N. Romano, M. Fanelli, G.M. Del Papa, G. Scapigliati, L. Mastrolia, Histological and cytological studies on the developing thymus of sharpsnout seabream, Diplodus puntazzo, J. Anat. 194 (1999) 39–50, https://doi.org/10.1046/j.1469-7580.1999.19410039.x.
[129] J. Cao, Q. Chen, M. Lu, X. Hu, M. Wang, Histology and ultrastructure of the thymus during development in tilapia, Oreochromis niloticus, J. Anat. 230 (2017) 720–733, https://doi.org/10.1111/joa.12597.
[130] C.N. Miller, I. Proekt, J. von Moltke, K.L. Wells, A.R. Rajpurkar, H. Wang, K. Rattay, I.S. Khan, T.C. Metzger, J.L. Pollack, A.C. Fries, W.W. Lwin, E. J. Wigton, A.V. Parent, B. Kyewski, D.J. Erle, K.A. Hogquist, L.M. Steinmetz, R. M. Locksley, M.S. Anderson, Thymic tuft cells promote an IL-4-enriched medulla and shape thymocyte development, Nature 559 (2018) 627–631, https://doi.org/10.1038/s41586-018-0345-2.
[131] J. Sun, M. Li, Y. Xie, Y. Zhang, Y. Chai, Thymic tuft cells: potential "regulators" of non-mucosal tissue development and immune response, Immunol. Res. 71 (2023) 554–564, https://doi.org/10.1007/s12026-023-09372-6.
[132] G. Ferrero, E. Gomez, S. lyer, M. Rovira, M. Miserocchi, D.M. Langenau, J. Y. Bertrand, V. Wittamer, The macrophage-expressed gene (mpeg) 1 identifies a subpopulation of B cells in the adult zebrafish, J. Leukoc. Biol. 107 (2020) 431–443, https://doi.org/10.1002/JLB.1A1119-223R.
[133] J.E. Konkel, W. Jin, B. Abbatiello, J.R. Grainger, W. Chen, Thymocyte apoptosis drives the intrathymic generation of regulatory T cells, Proc. Natl. Acad. Sci. U.S. A. 111 (2014) 465–473, https://doi.org/10.1073/pnas.1320319111.
[134] S. Fu, N. Zhang, A.C. Yopp, D. Chen, M. Mao, D. Chen, H. Zhang, Y. Ding, J. S. Bromberg, TGF-β induces Foxp3+ T-regulatory cells from CD4+ CD25- precursors, Am. J. Transplant. 4 (2004) 1614–1627, https://doi.org/10.1111/j.1600-6143.2004.00566.x.
[135] L. Wu, Z. Qin, H. Liu, L. Lin, J. Ye, J. Li, Recent advances on phagocytic B cells in teleost fish, Front. Immunol. 11 (2020), https://doi.org/10.3389/fimmu.2020.00824.
[136] A.G. Granja, P. Perdiguero, A. Martín-Martín, P. Díaz-Rosales, I. Soleto, C. Tafalla, Rainbow trout IgM+ B cells preferentially respond to thymus-independent antigens but are activated by CD40L, Front. Immunol. 10 (2019), https://doi.org/10.3389/fimmu.2019.02902.
[137] J. Castañeda, Y. Hidalgo, D. Sauma, M. Rosemblatt, M.R. Bono, S. Núñez, The multifaceted roles of B cells in the thymus: from immune tolerance to autoimmunity, Front. Immunol. 12 (2021), https://doi.org/10.3389/fimmu.2021.766698.
[138] M.P. Lins, Thymic extracellular matrix in the thymopoiesis: just a supporting? BioTech 11 (2022) https://doi.org/10.3390/biotech11030027.
[139] T. Nitta, M. Tsutsumi, S. Nitta, R. Muro, E.C. Suzuki, K. Nakano, Y. Tomofuji, S. Sawa, T. Okamura, J.M. Penninger, H. Takayanagi, Fibroblasts as a source of self-antigens for central immune tolerance, Nat. Immunol. 21 (2020) 1172–1180, https://doi.org/10.1038/s41590-020-0756-8.
[140] W. Savino, S.D. Silva-Barbosa, Laminin/VLA-6 interactions and T cell function, Braz. J. Med. Biol. Res. 29 (1996) 1209–1220.
[141] L. Muhl, G. Genové, S. Leptidis, J. Liu, L. He, G. Mocci, Y. Sun, S. Gustafsson, B. Buyandelger, I.V. Chivukula, Å. Segerstolpe, E. Raschperger, E.M. Hansson, J.L. M. Björkegren, X.R. Peng, M. Vanlandewijck, U. Lendahl, C. Betsholtz, Single-cell analysis uncovers fibroblast heterogeneity and criteria for fibroblast and mural

cell identification and discrimination, Nat. Commun. 11 (2020), https://doi.org/10.1038/s41467-020-17740-1.

[142] R.S. Resop, C.H. Uittenbogaart, Human T-cell development and thymic egress: an infectious disease perspective, Forum Immunopathol. Dis. Ther. 6 (2015) 33–49, https://doi.org/10.1615/ForumImmunDisTher.2015014226.

[143] A. Flávia Nardy, L. Santos, C.G. Freire-de-Lima, A. Morrot, Modulation of intrathymic sphingosine-1-phosphate levels promotes escape of immature thymocytes to the periphery with a potential proinflammatory role in chagas disease, BioMed Res. Int. 2015 (2015) 1–6, https://doi.org/10.1155/2015/709846.

[144] A. Miccoli, S. Picchietti, A.M. Fausto, G. Scapigliati, Evolution of immune defence responses as incremental layers among Metazoa, Eur. Zool. J. 88 (2021) 44–57, https://doi.org/10.1080/24750263.2020.1849435.

[145] G. Scapigliati, A.M. Fausto, S. Picchietti, Fish lymphocytes: an evolutionary equivalent of mammalian innate-like lymphocytes? Front. Immunol. 9 (2018) 1–8, https://doi.org/10.3389/fimmu.2018.00971.